THE UNIVERSITY OF MANITOBA

HIGH-Q ACTIVE RC BAND PASS FILTERS
USING TWO OPERATIONAL AMPLIFIERS

by

SIRUS SADUGHI

A Thesis
Submitted to The Faculty of Graduate Studies
In Partial Fulfillment of the Requirements for the Degree
of Master of Science

Department of Electrical Engineering

Winnipeg, Manitoba

February 1979

HIGH-Q ACTIVE RC BAND PASS FILTERS

USING TWO OPERATIONAL AMPLIFIERS

BY

SIRUS SADUGHI

A dissertation submitted to the Faculty of Graduate Studies of the University of Manitoba in partial fulfillment of the requirements of the degree of

MASTER OF SCIENCE

ABSTRACT

Three new second order band pass filters are presented. Two of them are based on negative impedance converter techniques which have one and two operational amplifiers in their realizations. The single amplifier realization has better characteristics than a comparable Sallen and Key type, while the two-amplifier realization is superior to conventional RC-NIC filters from the sensitivity point of view. The third realization is a versatile multiple feedback filter which exhibits improved frequency response, reasonable Q-sensitivities, capability of independent tuning of ω_o, Q and R_{in}, and wide dynamic range. Experimental results are provided to support the viability of the proposed filters.

ACKNOWLEDGEMENTS

I wish to express my deep gratitude to Dr. H.K. Kim for his untiring supervision and encouragement. Thanks are due to Professor M. Yunik and Dr. J.S. Townsend for reviewing the manuscript as committee members, especially Professor M. Yunik, my coadvisor, for his helpful suggestions.

CONTENTS

CHAPTER I

INTRODUCTION

Active RC filters were first introduced in the thirties. Due to the bulky size of vacuum tubes, however, they were of little practical use. The situation changed dramatically in the advent of solid state components in the late forties. Research and development efforts in active filters in recent years have been influenced primarily by the progress and breakthroughs in linear microelectronic circuit technology. The reduction of size, weight, power consumption and an increase in electronic system reliability are the main factors for producing active filters in microelectronic form. Because of the inexpensive price of active elements (transistors and operational amplifiers), the addition of these elements in RC filters does not increase price significantly any longer. The application of active RC filters in industry is common in many areas such as consumer electronics, communication systems and precision instruments. The primary application of active RC filters is at relatively low frequencies where inductors are not suitable because of their bulky size and low quality. With presently available commercial operational amplifiers the useful frequency is roughly from dc to 500 kHz. Compared to the more conventional LC filters, active RC filters tend to be smaller in size and cheaper at lower frequencies.

There are various active RC realizations of filters using operational amplifiers. Because filters were specifically designed for different characteristics such as sensitivity, component count, stability, frequency response, dynamic range, gain, input and output impedance, etc., they are quite numerous. The purpose of this thesis is to investigate new types of band pass filters with better sensitivity and frequency response characteristics. Modern active network synthesis started by using negative impedance converters as a network element. These filter realizations proved to be highly sensitive to element changes. The other approaches were proposed later, using impedance inverters and converters, such as gyrators or Frequency Dependent Negative Resistors. Until state variable filters were introduced, many filters based on RC-amplifier coefficient matching technique were reported. They all failed to meet some of the specifications in practical filters and are therefore special purpose types. State variable filters proved to be the best but lacked frequency response. This thesis is an attempt to circumvent some of the shortcomings in realizing band pass filters discussed above. Chapter II reviews these methods of filter realizations, while Chapter III introduces several new configurations together with their characteristics and includes some experimental results.

CHAPTER II

GENERAL FILTER DESIGN

Active RC filter design begins with the approximation of the specified network transfer characteristic as a real rational transfer function in the complex frequency variable s, in the form of

$$T(s) = \frac{a_n s^n + a_{n-1} s^{n-1} + \ldots + a_1 s + a_o}{b_m s^m + b_{m-1} s^{m-1} + \ldots + b_1 s + b_o} \qquad n \leq m \tag{2.1}$$

where m is the order of filter.

There are basically two approaches to filter design. In the direct realization approach, the filter transfer function given in (2.1) is synthesized in a manner similar to the passive filter synthesis using two ports. In the cascade realization approach the filter is synthesized as a tandem connection of second order filters. The transfer function T(s) in (2.1) can be decomposed into second order transfer functions $T_1(s)$, $T_2(s)$, ... , $T_k(s)$

$$T(s) = \prod_{j=1}^{k} T_j(s) \tag{2.2}$$

where $k = \frac{m}{2}$ m even

$k = \frac{m+1}{2}$ m odd, then T_k is first order.

Each second order term has the form

$$T_j(s) = K_j \frac{s^2 + \alpha_{j1} s + \alpha_{jo}}{s^2 + \beta_{j1} s + \beta_{jo}} \tag{2.3}$$

where $Q_j = \frac{\sqrt{\beta_{jo}}}{\beta_{j1}}$, $\omega_{oj} = \sqrt{\beta_{jo}}$.

The a_i and b_i for the network transfer function T(s) in (2.1) are real and hence the poles and zeros of T(s) are either real or occur in complex conjugate pairs. Since the poles of T(s) are in the left half plane, the βs are all positive. In other words, the denominator polynomial is strictly Hurwitz. On the other hand the αs may assume any real value including negative and zero depending on the location of the transmission zeros. The pairing of poles and zeros for the optimization of certain design criteria is itself an interesting problem but we shall assume that (2) and (3) are obtained. In general each block realizing T_j must be isolated from the ensuing block by means of a buffer amplifier. This implies an increase in the number of required amplifiers. However, easy access to inexpensive active elements, particularly operational amplifiers, justifies multi-amplifier design provided that improvement in performance is attainable. In general, low sensitivities, easy tunability, high-Q realizability are prominent features associated with multi-amplifier configurations.

2.1 Realization techniques

There are several methods for filter realizations. They include use of simulated inductance, frequency dependent negative resistor, RC-amplifier coefficient matching technique, generalized impedance converter, and state space method.

2.1.1 Simulated inductance or gyrator filters

In this type of filter, the transfer function is synthesized by a passive RLC network and then RC active netowrks simulating the inductors are embedded in place of inductors in the original passive network. The gain is always less than unity because of passivity of this kind of filter. The final design however is not simple. Since the output is taken from the passive network, a loading effect appears unless each section is perfectly matched. In general, two active elements are necessary for each inductance simulation. Gyrator filters are mainly used in moderate-Q high order filter realizations. The complexity of design is the same as in passive RLC designs and because of this similarity, the sensitivities are relatively low. The required number of components is high and specially in a cascade realization number of active elements increases. Several circuits are available for inductance simulation. They are basically impedance inverters which of course will have high frequency limitations due to the phase shift in the active elements. A typical of these circuits is Riordan gyrator [2] given in Fig. 2.1.

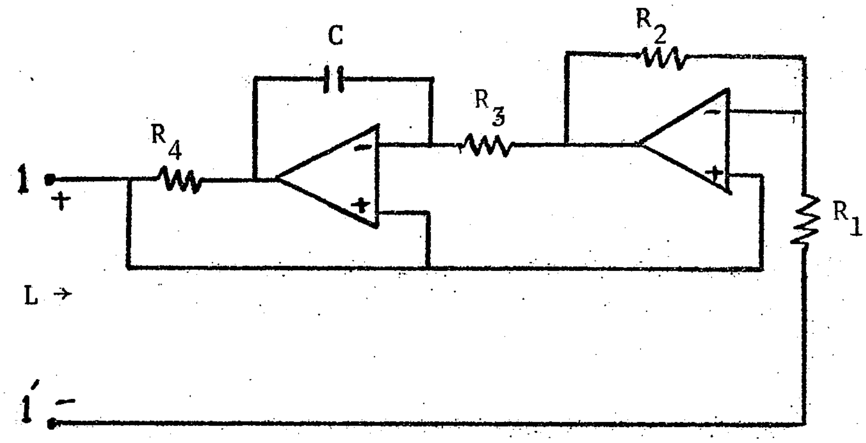

Fig. 2.1 Riordan gyrator

The input impedance at the terminals 11′, is approximately that of an inductance with a value of $L = \frac{R_1R_3R_4}{R_2}C$. The quality of this inductor is dependent on circuit parameters, however with $R_1=R_2$ and $\omega R_3C = 1$, it is possible to obtain high quality inductor at low frequencies, but due to phase shift in the operational amplifiers at high frequencies, subsequent instability may result.

2.1.2 Filters using Frequency Dependent Negative Resistors

This type of filter is obtained by transforming the network comprised of R, L, and C to another network with C, R, and a new element D. This new element is called Frequency Dependent Negative Resistor (FDNR) and has an input impedance equal to $\frac{1}{Ds^2}$. The transformation is obtained by dividing the impedances by s, and then a resistor transforms into a capacitor and an inductor transforms into a resistor and the capacitor into D.

A typical circuit realizing an FDNR is shown in Fig. 2.2.

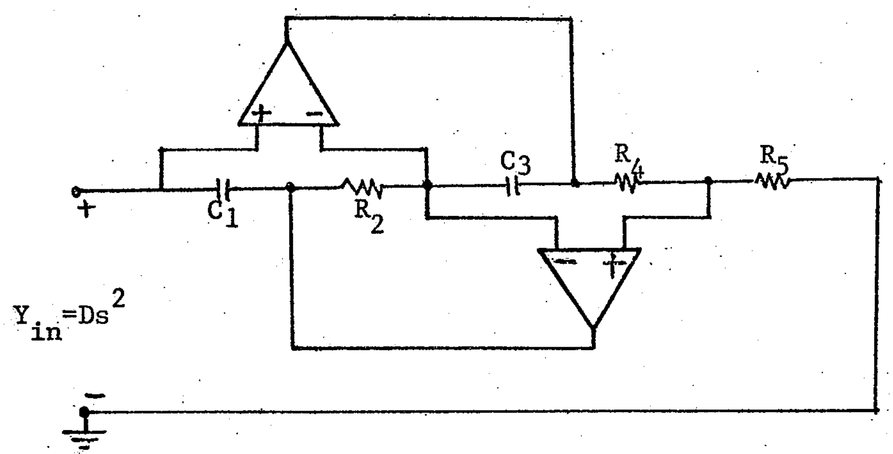

Fig. 2.2 Circuit realization of an FDNR

It can be shown that D in the above realization is given by

$D = \frac{R_2R_4C_1C_3}{R_5}$ provided that the operational amplifiers are ideal.

A filter using FDNRs works best when all the capacitors in the original network are grounded, which in turn results in grounded FDNRs. Therefore, this type of filter realization is suitable for high order low pass filters. Floating FDNRs are also realizable, but they are potentially unstable.

The complexity of design is the same as that of gyrator filters. Cascade realization is rarely used because there would be more passive and active elements. FDNR filters or in general positive impedance converter (PIC) filters exhibit the same characteristics as gyrator filters. Briefly, they have limited frequency response and a limited Q. Sensitivities are low, as well as the gain which is less than unity. In addition they use a large number of passive components.

2.1.3 RC-Amplifier realization

There are a number of circuits composed of R, C, and operational amplifiers, which realize general or special forms of transfer functions. The synthesis is based on coefficient matching and pole-zero cancellation is usually necessary to produce desired transfer function. Hence the number of components is high and for the minimal case, the number of capacitors used, is equal to the order of transfer function. The number of amplifiers in these kinds of filters is important and canonic types are defined on that basis. A typical filter in this category, using one OP-Amp, is the "Infinite gain realization" filter, which is shown in Fig. 2.3.

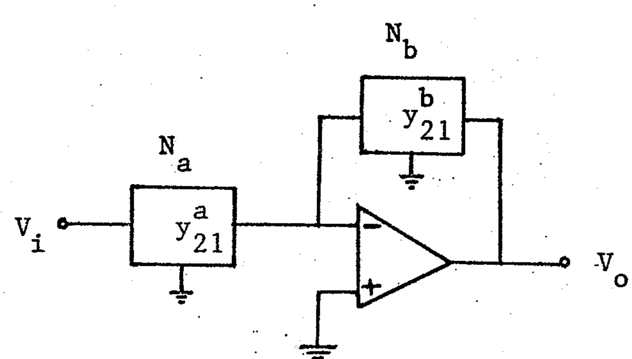

Fig. 2.3 Infinite gain realization of a transfer function

The voltage transfer function is given by

$$\frac{V_o}{V_i} = -\frac{y_{21}^a}{y_{21}^b} \tag{2.4}$$

where y_{21}^a and y_{21}^b are the short circuit transfer admittance of networks N_a and N_b. Figure 2.4 is the canonic realization of a second order band pass filter using the above configuration.

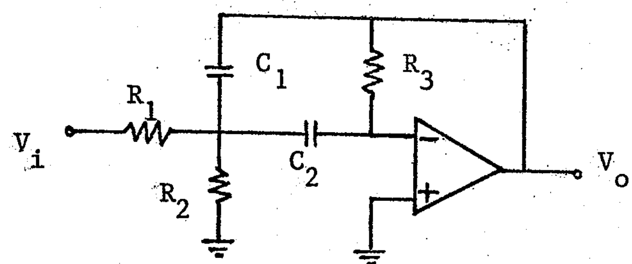

Fig. 2.4 Canonical form of infinite gain realization of a second order band pass filter

2.1.4 Generalized impedance converter method

In this type of realization, the transfer function is partitioned into RC realizable subnetworks connected by generalized impedance converter. Examples for RC-Gyrator and RC-NIC (negative impedance converter) realizations of second order low pass filters are given in Fig. 2.5.

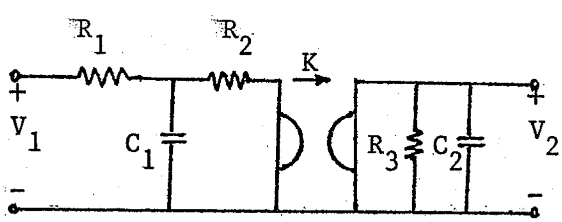

(a)

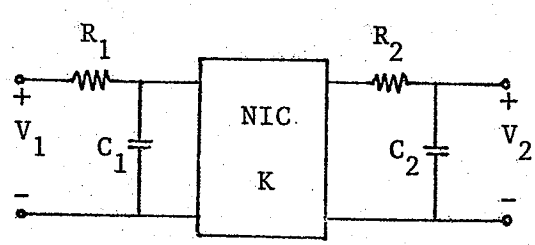

(b)

Fig. 2.5 RC-Gyrator (a) and RC-NIC (b) realizations of a second order low pass filter.

The technique employed in the realization is in fact RC:RL decomposition for RC-Gyrator type and RC:-RC decomposition for RC-NIC type. Both methods are cascade realizations and it should be mentioned that parallel realizations are also possible. The method of decomposition determines the sensitivity of transfer function to circuit parameters. There are optimal decompositions in both types which yield minimum sensitivities. [3] and [4].

2.1.5 State variable method

This method of realization is based on analog simulation of the transfer function using integrators, invertors and summing amplifiers. This type of filter is suitable for high Q realizations and amenable for easy tuning and low sensitivity. A large number of active elements are required and the nonidealness of these amplifiers results in a moderate frequency response.

The design procedure starts with determining the signal flow graph of the transfer function. An example of the method is given in [5]. The resulting analog computer simulation can be constructed by means of integrators, invertors and summing amplifiers. Figure 2.6 shows the signal flow graph and analog computer realization for a second order band pass filter; $\frac{V_2}{V_1} = \frac{\omega_o s}{s^2 + \frac{\omega_o}{Q} s + \omega_o^2}$.

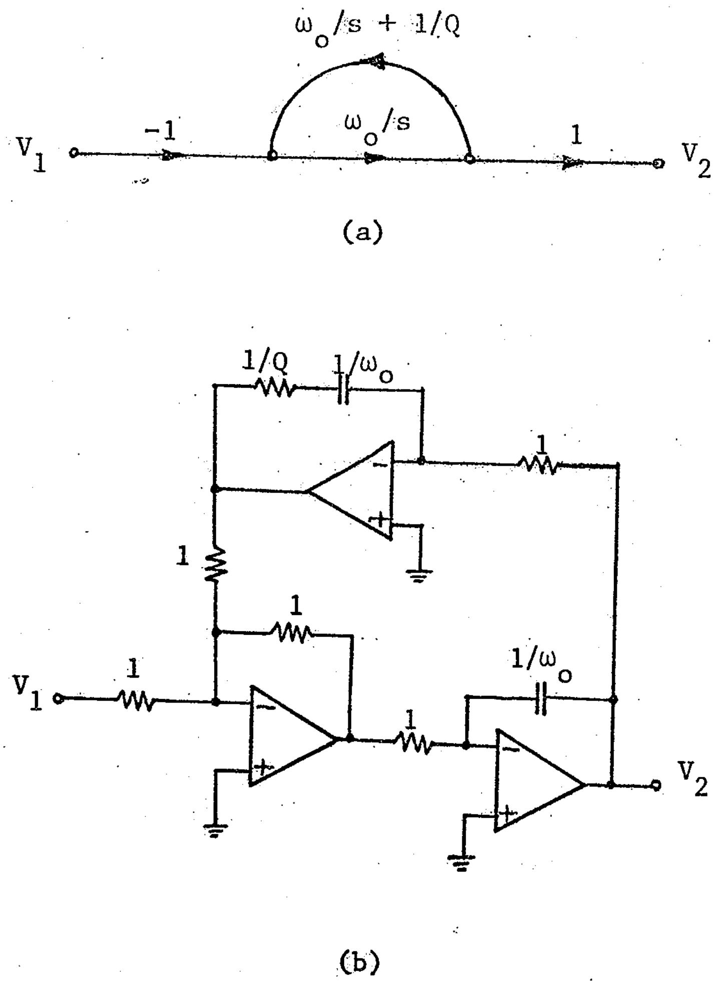

Fig. 2.6 (a) A signal flow graph realizing the second order band pass filter

(b) An analog-computer realization of (a)

2.2 Single amplifier realization of second order band pass filters

All the previous methods of filter realization require at least two operational amplifiers except the RC-Amplifier coefficient matching technique which follows.

2.2.1 RC-Amplifier realization

Different single amplifier structures can be classified as negative feedback (NF) and positive feedback (PF) configurations [6], as shown in Figs. 2.7(a) and 2.7(b).

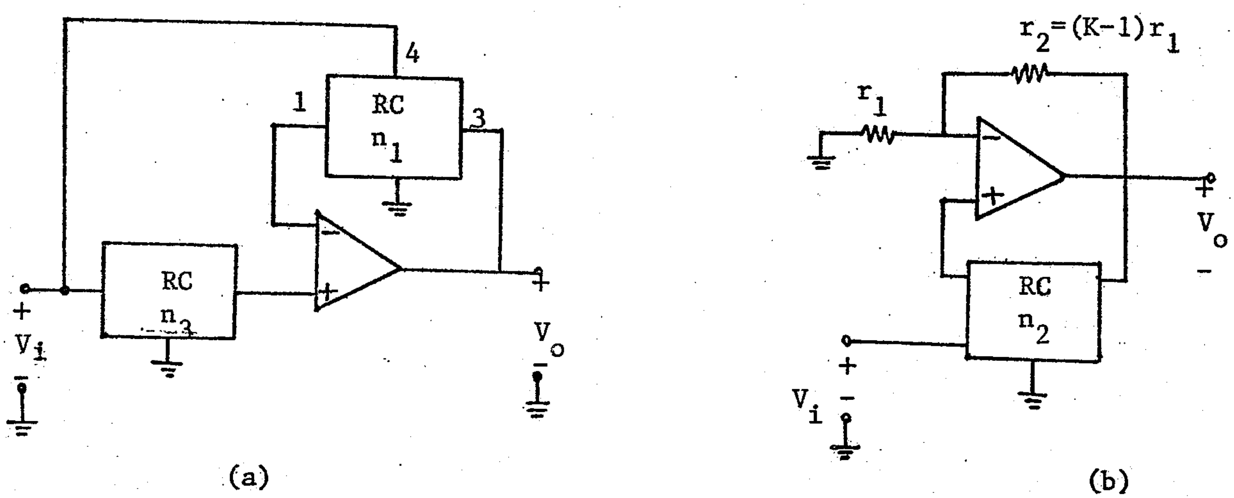

Fig. 2.7 NF(a) and PF(b) configurations for single amplifier transfer function realizations.

Positive feedback filters require a low gain amplifier and result in high Q-sensitivities, and wide bandwidth. On the other hand, negative feedback filters require high gain amplifier and yield low Q-sensitivities and narrower bandwidth. In both, NF or PF configurations, the type of RC network employed, determines the sensitivity properties of resulting filter.

Table 1 represents the characteristics of the various classes of filters.

Table 1

CLASS	PASSIVE Q-SENSITIVITIES	GAIN-SENSITIVITY PRODUCT	MAX. ELEMENT SPREAD
NF	Low	Q^2	Q^2
PF $K > 1$	Q	Q	Independent of Q
PF $K = 1$	Low	Q^2	Q^2

It has been shown that a better measure for active Q-sensitivities is the Gain Sensitivity Product GS^Q [7] defined as

$$GS_A^Q = AS_A^Q \tag{2.5}$$

where A is the amplifier gain and S_A^Q is the Q-sensitivity with respect to A. This measure becomes more meaningful when S_A^Q approaches zero figuratively due to extremely large value of A. This is the case for operational amplifier gain. Using the definition for sensitivity

$$\frac{\Delta Q}{Q} = S_A^Q \cdot \frac{\Delta A}{A} \quad . \tag{2.6}$$

If Q is a function of A, then it can be expanded in a Taylor series of the form

$$Q(\tfrac{1}{A}) = Q(0) + \frac{1}{A} \left. \frac{dQ}{d(\frac{1}{A})} \right|_{\frac{1}{A}=0} + \ldots\ldots \quad . \tag{2.7}$$

Truncating the series after the first two terms yields

$$Q(A) = Q_1 + \frac{Q_2}{A} \quad . \tag{2.8}$$

It is apparent that Q_1 and Q_2 are independent of A and depend only on the network. Calculating the Q-sensitivity with respect to A yields

$$S_A^Q = \frac{A}{Q} \cdot \frac{\partial Q}{\partial A} = \frac{A}{Q} \cdot \frac{-Q_2}{A^2} = \frac{-Q_2/Q}{A} \quad . \tag{2.9}$$

Thus
$$\lim_{A\to\infty} S_A^Q = 0 \tag{2.10}$$

and
$$GS_A^Q = AS_A^Q = -\frac{Q_2}{Q} \tag{2.11}$$

which is nonzero.

GS^Q or in general GSP is a well-defined analytical expression irrespective of whether A is finite or infinite. Thus minimizing GSP optimizes the sensitivity of the network irrespective of the sensitivities alone.

G.S. Moschytz and P. Horn [7] concluded that the effect of finite operational amplifier gain bandwidth product on pole-ω_o and pole-Q can be expressed in terms of GSP. This interesting result predicts the high frequency limitations of NF and PF configurations. Examples of canonic single amplifier NF and PF realizations are infinite gain multiple feedback filter and Sallen and Key filter, respectively.

Figures 2.8(a) and 2.8(b) are the realizations of a second order band pass filter by these two methods.

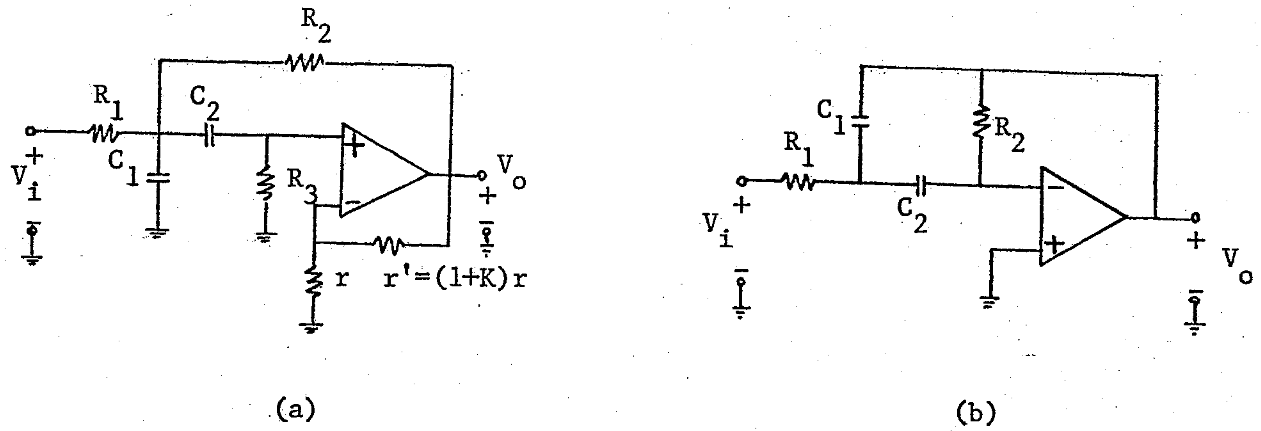

Fig. 2.8 (a) Sallen and Key; (b) Infinite gain multiple-feedback realizations of a second order band pass filter.

We shall investigate these two filters more in detail because they form an important base for the development in Chapter III

2.2.1 (a) Sallen and Key, second order band pass filter

The transfer function of this filter shown in 2.8(a) can be obtained as

$$T(S) = \frac{V_o}{V_i} = \frac{Ks/R_1C_1}{s^2+s\left(\frac{1}{R_1C_1}+\frac{1}{R_3C_2}+\frac{1}{R_3C_1}+\frac{1-K}{R_2C_1}\right)+\frac{R_1+R_2}{R_1R_2R_3C_1C_2}} \quad . \tag{2.12}$$

The resonance frequency ω_o and quality factor Q are

$$\omega_o = \sqrt{\frac{R_1+R_2}{R_1R_2R_3C_1C_2}}\,, \qquad Q = \frac{\sqrt{\frac{R_2C_1(R_1+R_2)}{R_1R_3C_2}}}{1+\frac{R_2}{R_1}+\frac{R_2}{R_3}\left(1+\frac{C_1}{C_2}\right)-K} \quad . \tag{2.13}$$

For equal-R, equal-C, we have

$$\omega_o = \frac{\sqrt{2}}{RC}\,, \qquad Q = \frac{\sqrt{2}}{4-K} \quad . \tag{2.14}$$

The ω_o and Q sensitivities are

$$S_{R_1}^{\omega_o} = S_{R_2}^{\omega_o} = -\frac{1}{4},\quad S_{R_3}^{\omega_o} = S_{C_1}^{\omega_o} = S_{C_2}^{\omega_o} = -\frac{1}{2},\quad S_K^{\omega_o} = 0 \tag{2.15}$$

$$S_{R_1}^{Q} = -\frac{1}{4}+\frac{1}{\sqrt{2}}Q,\quad S_{R_2}^{Q} = \frac{3}{4}-\frac{3}{\sqrt{2}}Q,\quad S_{R_3}^{Q} = -\frac{1}{2}+\sqrt{2}\,Q$$

$$S_{C_1}^{Q} = -S_{C_2}^{Q} = \frac{1}{2}-\frac{1}{\sqrt{2}}Q,\quad S_K^{Q} = 2\sqrt{2}\,Q-1 \tag{2.16}$$

$$GS^Q = KS_K^Q = 8\sqrt{2}\,Q - 8 + \frac{\sqrt{2}}{Q} \simeq 8\sqrt{2}\,Q \qquad (Q\gg 1) \quad . \tag{2.17}$$

The effect of finite operational amplifier gain bandwidth product on the performance of this filter is given in [8]. The ω_o and Q variations are

$$\frac{\Delta\omega_o}{\omega_c} \simeq -4\sqrt{2}\,\frac{\omega_o}{GB}\ ,\ \frac{\Delta Q}{Q} \simeq 4\sqrt{2}\,\frac{\omega_o}{GB}\ \text{provided that } Q>>1 \tag{2.18}$$

where GB is the gain bandwidth product of the operational amplifier.

We can also obtain (2.18) by two explicit approximation formulas given in [9]

$$\delta \equiv \frac{\Delta\omega_o}{\omega_o} \simeq \frac{1}{2}\ \frac{\omega_o}{GB}\,\frac{1}{Q}\ (GS_K^Q)$$

$$\frac{\Delta Q}{Q} \simeq \frac{-\delta+4Q\delta\frac{\omega_o}{GB}}{1+\delta-4Q\delta\frac{\omega_o}{GB}} \tag{2.19}$$

The gain sensitivity product for this filter is equal to approximately $8\sqrt{2}Q$ thus

$$\frac{\Delta\omega_o}{\omega_o} \simeq -\frac{1}{2}\,\frac{\omega_o}{GB}\cdot 8\sqrt{2} = -4\sqrt{2}\,\frac{\omega_o}{GB}$$

$$\frac{\Delta Q}{Q} \simeq -\delta = 4\sqrt{2}\,\frac{\omega_o}{GB} \tag{2.20}$$

provided that $4Q\omega_o << GB$.

If ω_o and Q have large values then according to (2.19), the Q-variation is not in the order of δ but much higher. For example, if $\omega_o = 10^4$ and $Q = 100$, then $\delta = 0.055$ and $\frac{\Delta Q}{Q} = .2$.

The ω_o and Q variations due to operational amplifier finite gain bandwidth product were shown to be dependent on GB and GSP. Thus for minimizing these variations we require lower gain sensitivity product and a low frequency operation. Some of the drawbacks of this filter are the low input impedance, high gain at the resonance frequency and high (passive and active) Q-sensitivities. The input impedance and gain at resonance frequency are $-\frac{2}{3Q}R(\sqrt{2}+j)$ and $(2\sqrt{2}Q-1)$, respectively. Obviously, this filter is impractical for cascade realization of high-Q high order filters because of low input impedance and high gain.

2.2.1 (b) Infinite gain multiple feedback filter

The filter given in Fig. 2.8(b) has the following transfer voltage

$$T(s) = \frac{V_o}{V_i} = \frac{-\frac{1}{R_1C_1}s}{s^2+\frac{1}{R_2}(\frac{1}{C_1}+\frac{1}{C_2})s+\frac{1}{R_1R_2C_1C_2}} \quad . \qquad (2.21)$$

The ω_o and Q are

$$\omega_o = \frac{1}{\sqrt{C_1C_2R_1R_2}} \quad , \qquad Q = \frac{\sqrt{R_2/R_1}}{\sqrt{C_1/C_2}+\sqrt{C_2/C_1}} \quad . \qquad (2.22)$$

For the case $C_1 = C_2 = C$ we have

$$\omega_o = \frac{1}{C\sqrt{R_1R_2}} \quad , \qquad Q = \frac{1}{2}\sqrt{\frac{R_2}{R_1}} \quad . \qquad (2.23)$$

The ω_o and Q sensitivities are

$$S_{R_1}^{\omega_o} = S_{R_2}^{\omega_o} = S_{C_1}^{\omega_o} = S_{C_2}^{\omega_o} = -\frac{1}{2}$$

$$S_{R_1}^{Q} = -S_{R_2}^{Q} = -\frac{1}{2}, \; S_{C_1}^{Q} = S_{C_2}^{Q} = 0 \quad . \qquad (2.24)$$

The sensitivities with respect to passive elements are low. To find the active Q sensitivity we substitute the one pole roll-off model for operational amplifier with the gain of A. Figure 2.9 illustrates this model for the nonideal Op-Amp.

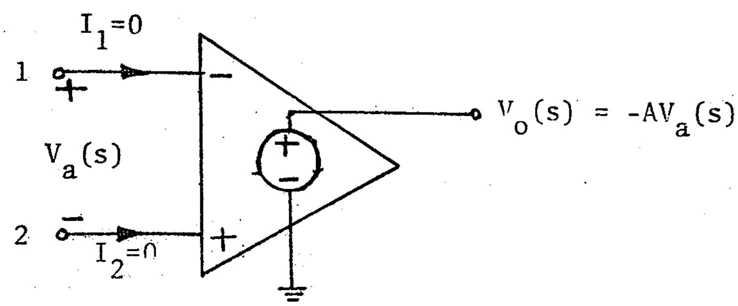

Fig. 2.9 One-pole roll off model for non-ideal operational amplifier

The gain of this amplifier is frequency dependent and equal to $A = \frac{GB}{s+\omega_a}$ where GB is the gain bandwidth product and ω_a is the 3dB down frequency of the operational amplifier. GB can also be written as $GB = A_o\omega_a$, where A_o is the dc open loop gain. Substituting the one pole roll-off model for the operational amplifier in the circuit of Fig. 2.8(b) yields

$$\frac{V_o}{V_i} = \frac{-R_2C_2s}{(1+\frac{1}{A})R_1R_2C_1C_2s^2 + [-R_2C_2+(1+\frac{1}{A})(R_2C_2+R_1C_1+R_1C_2)]s+1+\frac{1}{A}} \cdot \tag{2.25}$$

The Q and Q-sensitivity with respect to A are

$$Q_A = \frac{(1+\frac{1}{A})\sqrt{R_1R_2C_1C_2}}{-R_2C_2+(1+\frac{1}{A})(R_1C_1+R_2C_2+R_1C_2)} \tag{2.26}$$

if $C_2=C_1=C$, $R_2=4Q^2R_1$ then (2.26) reduces to

$$Q_A = \frac{Q(A+1)}{A+1+2Q^2} \tag{2.27}$$

with $$S_A^{Q_A} = \frac{2Q^2 A}{(A+1)(A+1+2Q^2)} \tag{2.28}$$

if $A \to \infty \Rightarrow \quad S_A^{Q_A} \to 0$.

But the GSP is finite as follows

$$GS_A^Q = AS_A^{Q_A} = \frac{2Q^2 A^2}{(A+1)(A+1+2Q^2)} \tag{2.29}$$

and if $A \to \infty$ then

$$GS_{A\to\infty}^Q = 2Q^2 \ . \tag{2.30}$$

Using (2.19) yields

$$\delta = \frac{\Delta\omega_o}{\omega_o} \simeq -\frac{1}{2}\,\frac{\omega_o}{GB}\,\frac{1}{Q}\cdot 2Q^2 = -Q\frac{\omega_o}{GB}$$

and $$\frac{\Delta Q}{Q} \simeq \frac{Q\frac{\omega_o}{GB} - 4Q^2\left(\frac{\omega_o}{GB}\right)^2}{1-Q\frac{\omega_o}{GB} + 4Q^2\left(\frac{\omega_o}{GB}\right)^2} \ . \tag{2.31}$$

If ω_o and Q have moderate values then we can ignore the terms containing GB^2 in $\Delta Q/Q$ and in that case it simplifies to $Q\frac{\omega_o}{GB}$, thus

$$\frac{\Delta\omega_o}{\omega_o} \simeq -Q\frac{\omega_o}{GB} \ , \qquad \frac{\Delta Q}{Q} \simeq Q\frac{\omega_o}{GB} \ . \tag{2.32}$$

The GSP for this filter is evidently much higher than that of Sallen and Key filter. Hence lower frequency response and higher sensitivity to operational amplifier parameters are expected. The input impedance and gain at resonance frequency are $R_1/2(1+j)$ and $2Q^2$ respectively. As in the case of the Sallen and Key filter, the low imput impedance and high gain make this filter impractical for high Q, higher order realizations.

2.3 Two-amplifier active RC realizations of second order band pass filters

In this section we consider the canonical networks (same number of capacitors) realizing the second order bandpass filters. We exclude Gyrator and FDNR filters because they require buffer amplifiers. We have however included RC-NIC realization of the filter because NICs can be constructed by only one operational amplifier , the second amplifier serves as an isolator. There are a number of canonical RC two-amplifier realizations for a second order band pass filter given in [6]. Among these eight networks, some of them have low input impedance or high gain sensitivity product or high resistance spread. Excluding those, there remains four networks which are given in Fig. 2.10.

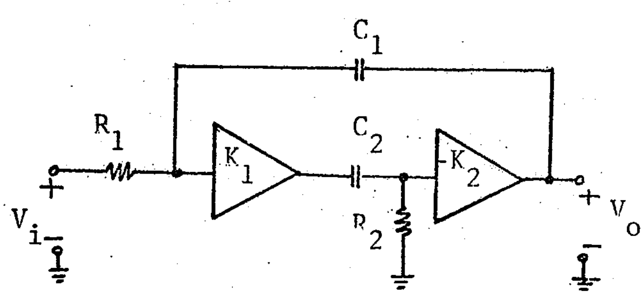

(a) $K_1K_2=4Q^2-1$, $C_1R_1=C_2R_2=\frac{1}{2\omega_oQ}$

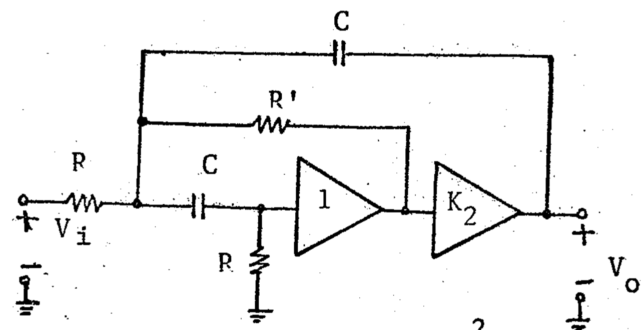

(b) $R'=R/\beta$, $CR=\frac{1+\beta}{3\omega_oQ}$, $K_2=\frac{9Q^2}{1+\beta}-1$

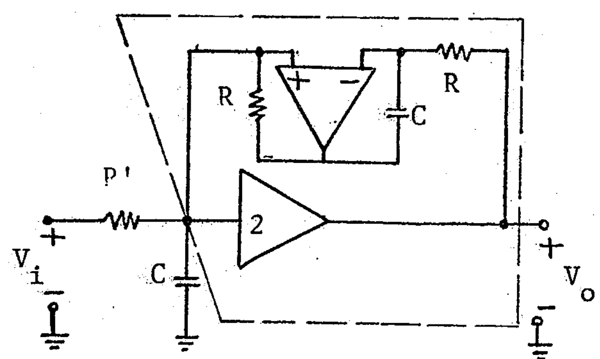

(c) $R' = QR$, $CR = \frac{1}{\omega_o}$

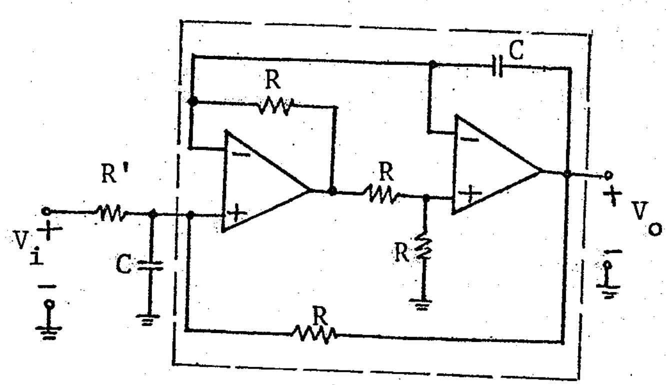

(d) $R' = QR$, $\omega_o = \frac{1}{RC}$

Fig. 2.10 Canonical two amplifier band pass filters

2.3a - The filter of Fig. 2.10(a) has low Q-sensitivities as well as low gain sensitivity products. Hence it has wide frequency response. Low input inpedance and high gain at resonance frequency which are $-j\ R_1/Q$ and $2Q^2$ respectively make this filter impractical for high Q, higher order realizations.

2.3b - The filter in Fig.2.10(b) has high gain sensitivity products unless β is chosen to be 3Q. The gain of this filter is $K_2/3$ or about $3Q^2/\beta$. As a result the gain is about Q which is high. Tuning of ω_o, Q, and gain cannot be done independently, consequently this filter lacks the practicality in high Q, higher order realizations.

2.3c-2.3d :

The circuits in Figs. 2.10(c) and 2.10(d) are both RC-L simulated filters. The parts of the circuits enclosed by broken lines simulate inductances. In Fig. 2.10(c), the input impedance of this port is Q^2R^2CS or the driving point impedance of an inductance with $L = Q^2R^2C$. In Fig. 2.10(d) the circuit has an input impedance of R^2CS which simulates an inductance whose value is R^2C. Because of the passivity of these filters the sensitivities are low. The maximum gain is 2. The frequency limitations of these filters are the same as state variable filter, since $\frac{\Delta\omega_o}{\omega_o} \simeq -\frac{\omega_o}{GB}$ and $\frac{\Delta Q}{Q} \simeq 4Q\,\frac{\omega_o}{GB}$.

Thus high Q, higher order realizations using these filters are not practical.

CHAPTER III

NEW ACTIVE RC REALIZATIONS OF BANDPASS FILTERS

In this chapter three second order band pass filters are presented. In Section 3.1 a single amplifier realization is considered which is based on the RC-negative impedance converter technique. Section 3.2 introduces another filter based on RC-NIC with negative load. Finally, in Section 3.3 a multiple feedback filter is developed which has properties suitable for high Q, high frequency realizations with reasonable sensitivity.

3.1 RC-NIC band pass filter realizations

For the canonical realization of an RC-NIC type of band pass filter we consider the cascade configuration shown in Fig. 3.1.

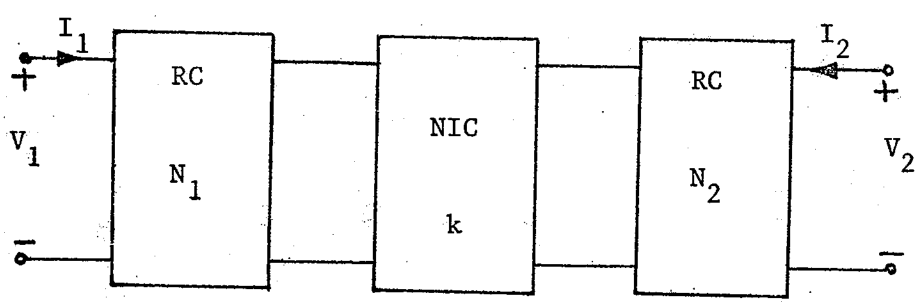

Fig. 3.1 Cascade configuration of an RC-NIC filter

The matrix equation describing circuit using transmission parameters is

$$\begin{bmatrix} V_1 \\ I_1 \end{bmatrix} = \begin{bmatrix} A_1 & B_1 \\ C_1 & D_1 \end{bmatrix} \begin{bmatrix} 1 & 0 \\ 0 & -\frac{1}{k} \end{bmatrix} \begin{bmatrix} A_2 & B_2 \\ C_2 & D_2 \end{bmatrix} \begin{bmatrix} V_2 \\ I_2 \end{bmatrix} \tag{3.1}$$

where $\begin{bmatrix} 1 & 0 \\ 0 & -\frac{1}{k} \end{bmatrix}$ is the transmission matrix for a current inversion negative impedance converter (CNIC). Alternately we could use a voltage inversion NIC (VNIC) with the transmission matrix $\begin{bmatrix} -\frac{1}{k} & 0 \\ 0 & 1 \end{bmatrix}$. Using the former, one obtains

$$\frac{V_2}{V_1} = \frac{1}{A_1A_2 - \frac{B_1C_2}{k}} \quad . \tag{3.2}$$

Networks N_1 and N_2 are chosen from four possibilities, shown in Fig. 3.2.

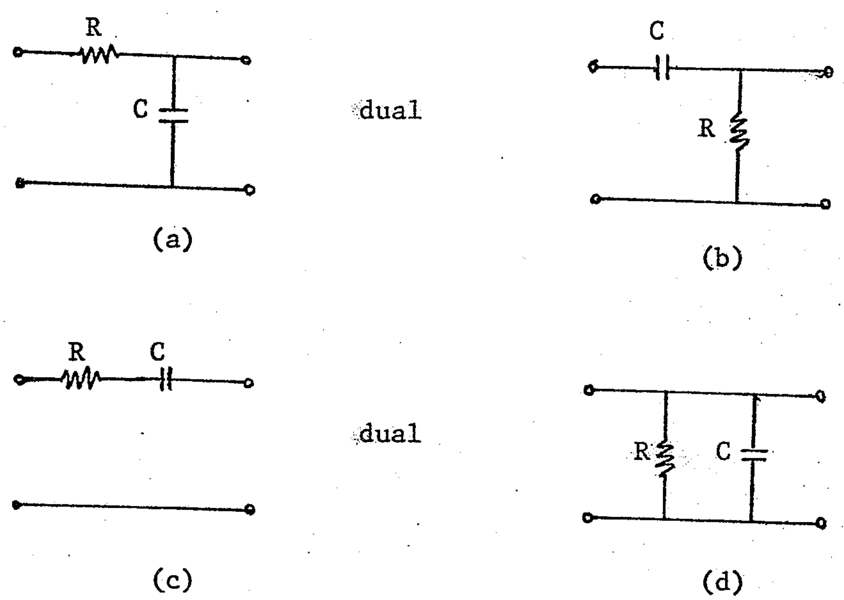

Fig. 3.2 Possible networks for a canonical second order filter

The corresponding transmission matrices for these configurations in Fig.3.2 are

$$\begin{bmatrix} 1+RCs & R \\ Cs & 1 \end{bmatrix} \tag{3.3a}$$

$$\begin{bmatrix} 1+\frac{1}{RCs} & \frac{1}{Cs} \\ \frac{1}{R} & 1 \end{bmatrix} \tag{3.3b}$$

$$\begin{bmatrix} 1 & R+\frac{1}{Cs} \\ 0 & 1 \end{bmatrix} \tag{3.3c}$$

$$\begin{bmatrix} 1 & 0 \\ \frac{1}{R}+Cs & 1 \end{bmatrix} \quad . \tag{3.3d}$$

Possible choices for networks N_1 and N_2 to yield a second order band pass filter are the pairs (a,b), (b,a) or (c,d) in (3.3).

The negative impedance converters which can be realized with one operational amplifier are shown in Fig. 3.3.

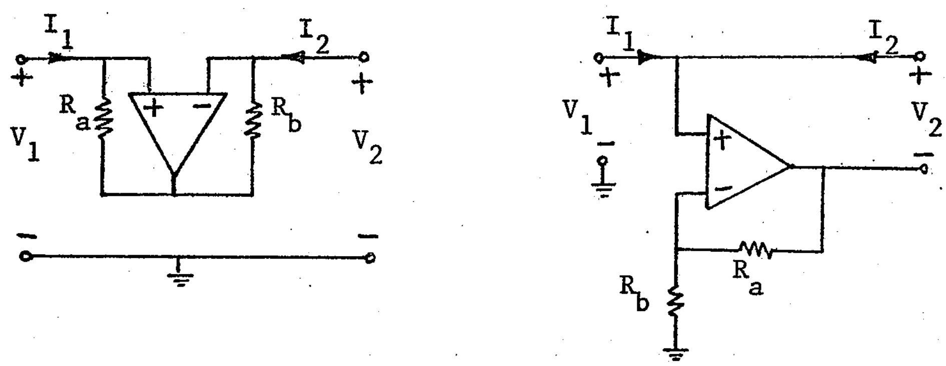

$V_2 = V_1$

$I_2 = -\frac{R_a}{R_b} I_1$

(a)

$I_1 = I_2$

$V_2 = -\frac{R_a}{R_b} V_1$

(b)

Fig. 3.3 Two realizations of NICs with $k = \frac{R_a}{R_b}$ (a) CNIC, (b) VNIC

For the RC-VNIC realization we obtain

$$\begin{bmatrix} V_1 \\ I_1 \end{bmatrix} = \begin{bmatrix} A_1 & B_1 \\ C_1 & D_1 \end{bmatrix} \begin{bmatrix} -\frac{1}{k} & 0 \\ 0 & 1 \end{bmatrix} \begin{bmatrix} A_2 & B_2 \\ C_2 & D_2 \end{bmatrix} \begin{bmatrix} V_2 \\ I_2 \end{bmatrix} \quad .$$

For open circuit gain we obtain

$$\frac{V_2}{V_1} = \frac{1}{-\frac{A_1 A_2}{k} + B_1 C_2} \quad . \tag{3.4}$$

The only possible configuration in Fig. 3.2 for producing a second order band pass filter is the pair (c,d) and as a result, we have the networks shown in Fig. 3.4.

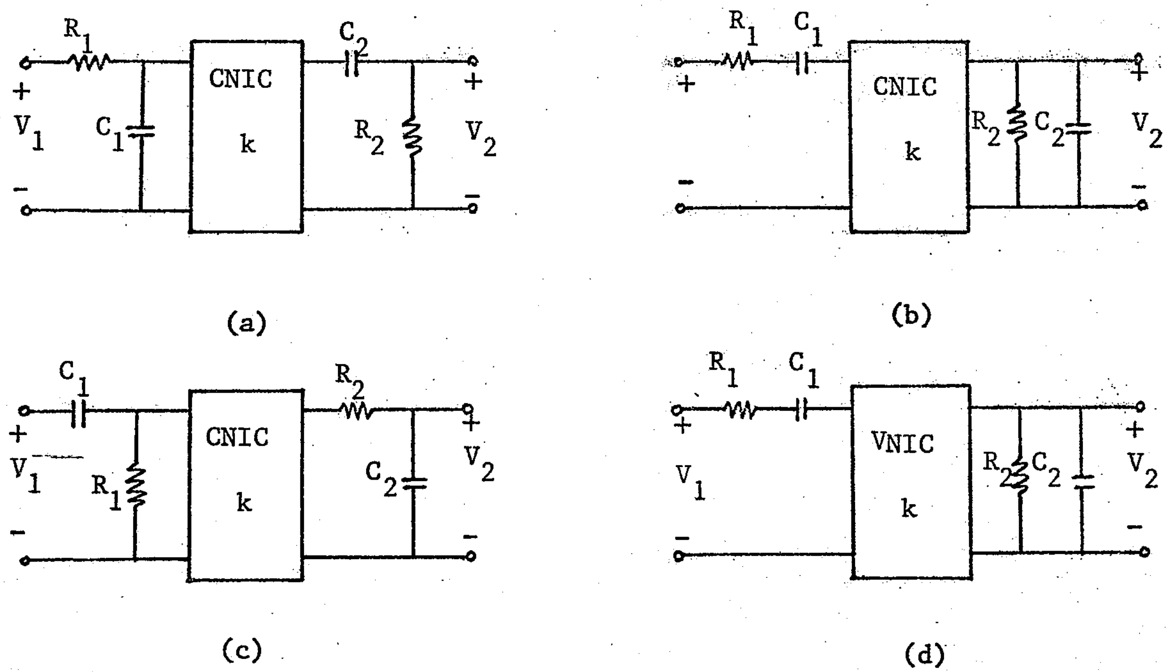

Fig. 3.4 Canonical RC-NIC realizations of four second order band pass filters

The two proposed circuits realizing the NIC are not strictly stable and care must be taken to insure proper connections to the subnetworks N_1 and N_2. Conditional stability of these circuits is due to the positive feedback provided by R_a to the operational amplifier positive terminal in CNIC and by the load in VNIC. To avoid instability, the amount of positive feedback should be decreased. This can be achieved by using a short circuit at the input port and an open circuit at the output in both circuits. For this reason the input port is called short circuit stable (SCS) and the output port open circuit stable (OCS). Due to the stability considerations, the circuits which are implementable are those given in Fig. 3.5.

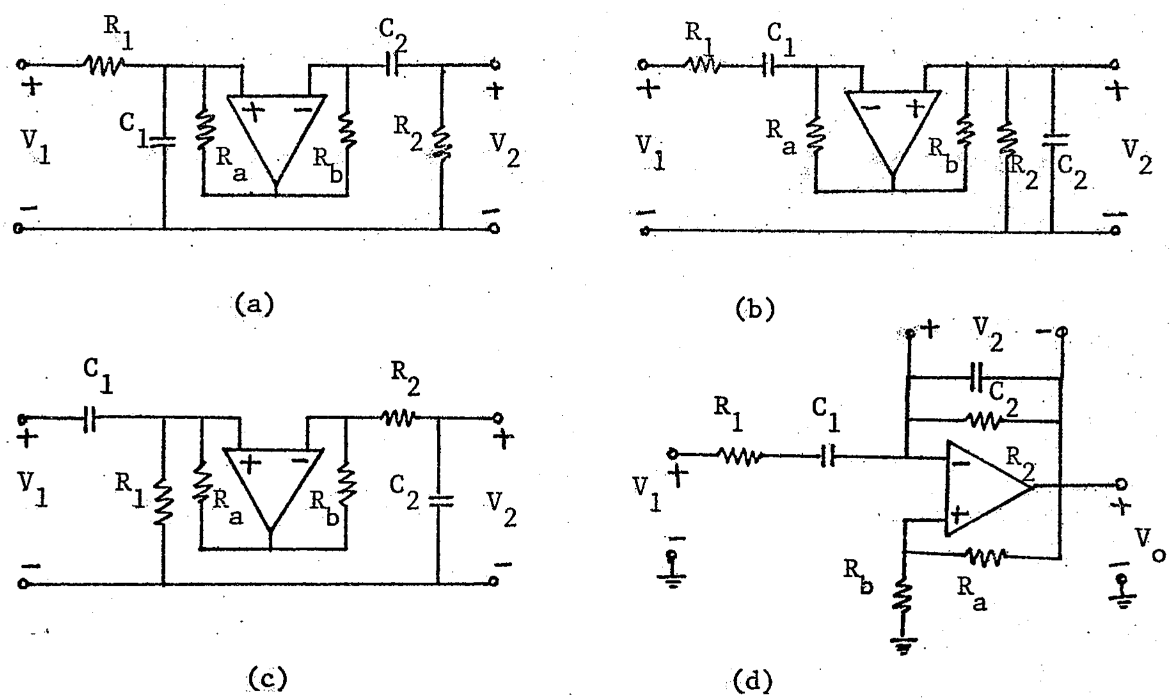

Fig. 3.5 Conditionally stable realizations of the networks in Fig. 3.4

3.1.1 Single amplifier realization

From Fig. 3.5(d), we have

$$V_2 = V_o \frac{R_b}{R_a+R_b} - V_o = V_o \frac{-R_a}{R_a+R_b} = -V_o \frac{1}{1+\frac{R_b}{R_a}} \qquad (3.5)$$

or $$V_o = -(1 + \frac{R_b}{R_a})V_2 = -(1 + \frac{1}{k})V_2 \quad . \qquad (3.6)$$

Thus the output of the operational amplifier is proportional to V_2 and therefore we can take the output of the filter from the V_o. The result is a single amplifier band pass filter. The other circuits however need a buffer amplifier and as a result they cannot be regarded as single amplifier filters. We shall consider the circuit in more detail.

For the circuit of Fig. 3.5(d), a straightforward analysis yields

$$\frac{V_2}{V_1} = \frac{R_2C_1s}{R_1R_2C_1C_2s^2 + (R_1C_2+R_2C_2-\frac{1}{k}R_2C_1)s + 1} \tag{3.7}$$

and since $V_o = -(1 + \frac{1}{k})V_2$, we have

$$\frac{V_o}{V_1} = -\frac{1+\frac{1}{k}}{R_1C_2}\,\frac{s}{s^2+(\frac{1}{R_2C_2} + \frac{1}{R_1C_1} - \frac{1}{k}\frac{1}{R_1C_2})s + \frac{1}{R_1R_2C_1C_2}} \tag{3.8}$$

where $\omega_o = \frac{1}{\sqrt{R_1R_2C_1C_2}}$, $Q = \frac{\sqrt{R_1R_2C_1C_2}}{R_1C_1+R_2C_2-\frac{1}{k}R_2C_1}$.

For equal-R, equal-C case, $\omega_o = \frac{1}{RC}$, $Q = \frac{1}{2-\frac{1}{k}}$

and their sensitivities are computed as follows

$$\begin{aligned} &S_{R_1}^{\omega_o} = S_{R_2}^{\omega_o} = S_{C_1}^{\omega_o} = S_{C_2}^{\omega_o} = -\frac{1}{2},\ S_k^{\omega_o} = 0 \\ &S_{R_1}^{Q} = -S_{R_2}^{Q} = S_{C_2}^{Q} = -S_{C_1}^{Q} = -Q + \frac{1}{2} \end{aligned} \tag{3.9}$$

$S_k^Q = 1-2Q$. Thus $S_{R_a}^Q = -S_{R_b}^Q = 1-2Q$

$\Sigma S_{Z_i}^Q = 0$, where Z_i represents every passive element.

This filter can be considered as a PF filter shown in Fig. 3.6.

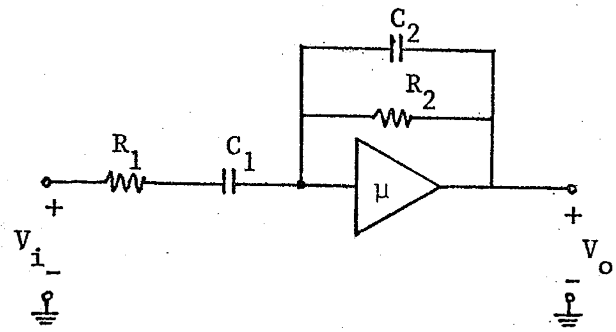

Fig. 3.6 RC-amplifier representation of the filter in Fig. 3.5(d)

With $\mu = 1+k$, the Q factor becomes

$$Q = \frac{k}{2k-1} = \frac{\mu-1}{2\mu-3}, \text{ hence}$$

$$S_{\mu}^{Q} = \frac{\mu}{Q} \cdot \frac{\partial Q}{\partial \mu} = -(3-\frac{1}{Q})(2Q-1). \tag{3.10}$$

If $Q \gg 1$ then $S_{\mu}^{Q} \simeq -6Q$

and the gain sensitivity product (GSP) for this filter becomes

$$GS_{\mu}^{Q} \simeq -6Q\mu \simeq -9Q \tag{3.11}$$

It is shown in [7] that

$$\mu S_{\mu}^{Q} = AS_{A}^{Q} = GSp \tag{3.12}$$

thus $GSP \simeq -9Q$.

By using (3.12) and (2.19), the ω_o and Q variations due to finite operational amplifier gain bandwidth product are computed as

$$\delta \doteq \frac{\Delta\omega_o}{\omega_o} \simeq -\frac{1}{2}\frac{\omega_o}{GB}\cdot\frac{1}{Q}\cdot(-9Q) \simeq 4.5\frac{\omega_o}{GB}$$

$$\frac{\Delta Q}{Q} \simeq -\delta = -4.5\frac{\omega_o}{GB}. \tag{3.13}$$

In terms of sensitivity and gain sensitivity product measures, it is evident that this filter is superior to Sallen and Key type filter.

The input impedance and gain at resonance frequency are $\frac{R}{2Q}(1-j)$ and $3Q-1$ which are roughly comparable to Sallen and Key filter. From the practical point of view, this filter is not suitable for high Q, high order realizations, because of high gain and high Q sensitivities.

3.1.2 Two-amplifier realizations with minimized sensitivity

Looking back to the other filters given in Fig. 3.5, we notice that they have similar voltage transfer functions and input impedances. There are several decomposition techniques such as the Horowitz decomposition [3] that minimize the pole-Q sensitivity but nevertheless it is greater than $(Q-\frac{1}{2})$ [11].

For the three filters in Fig. 3.5, the Q-sensitivities are

$$S^Q_{Z_i} = \pm(Q - \tfrac{1}{2}) \qquad Z_i = R \text{ or } C$$

$$S^Q_k = 2Q-1 \tag{3.14}$$

$$\Sigma S^Q_{Z_i} = 0 .$$

Thus we can neglect the minimum sensitivity decomposition for these filters, provided that the Q-sensitivities do not exceed $(Q-\frac{1}{2})$. This minimized value of $S^Q_{Z_i}$ only applies to passive elements. The Q-sensitivity with respect to conversion factor K is $(2Q-1)$. All these three networks in

Fig. 3.5 need a buffer amplifier to avoid the loading effect. By assuming a negative input resistance for the buffer amplifier we may achieve lower Q sensitivities.

The filter in Fig. 3.5(b) is amenable for this purpose. Fig. 3.7 shows this filter loaded with a negative resistor.

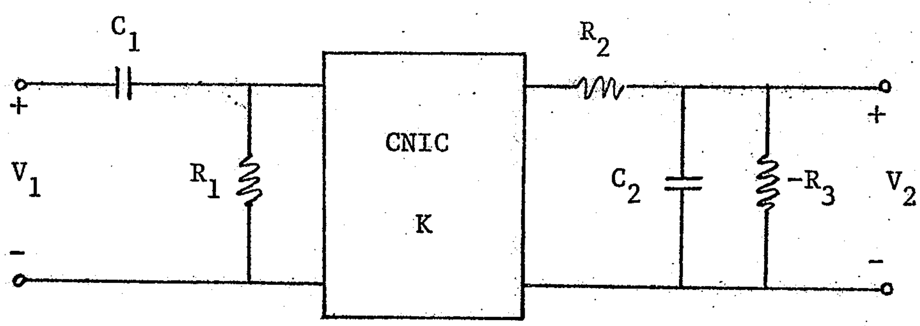

Fig. 3.7 RC-NIC realization of a band pass filter with negative load

The voltage transfer function of this filter is

$$\frac{V_2}{V_1} = \frac{R_1C_1s}{R_1R_2C_1C_2s^2 + [(1-R_2G_3)R_1C_1 + (R_2-KR_1)C_2]s + 1-R_2G_3+K_1R_1G_3} \qquad (3.15)$$

with $\omega_o = \sqrt{\dfrac{1-R_2G_3+KR_1G_3}{R_1R_2C_1C_2}}$ and $Q = \dfrac{\sqrt{(1-R_2G_3+KR_1G_3)(R_1R_2C_1C_2)}}{(1-R_2G_3)R_1C_1+(R_2-KR_1)C_2}$.

The Q sensitivities are

$$S^Q_{C_1} = \frac{1}{2} - \frac{(1-R_2G_3)R_1C_1}{(1-R_2G_3)R_1C_1+(R_2-KR_1)C_2}$$

$$S^Q_{C_2} = \frac{1}{2} - \frac{(R_2-KR_1)\ C_2}{(1-R_2G_3)R_1C_1+(R_2-KR_1)C_2}$$

$$S^Q_{R_2} = \frac{1}{2} - \frac{R_2G_3}{2(1-R_2G_3+KR_1G_3)} - \frac{(C_2-R_1G_3C_1)R_2}{(1-R_2G_3)R_1C_1+R_2C_2-KR_1C_2} \tag{3.16}$$

$$S^Q_{R_1} = \frac{1}{2} + \frac{KR_1G_3}{2(1-R_2G_3+KR_1G_3)} - \frac{(1-R_2G_3)R_1C_1-KR_1C_2}{(1-R_2G_3)R_1C_1+(R_2-KR_1)C_2}$$

$$S^Q_{R_3} = \frac{-(R_2-KR_1)G_3}{2(1-R_2G_3+KR_1G_3)} + \frac{R_2G_3R_1C_1}{(1-R_2G_3)R_1C_1+(R_2-KR_1)C_2} .$$

If the resistors and capacitors are equal valued then

$$\frac{V_2}{V_1} = \frac{\frac{1}{RC}\,s}{s^2+(1-K)\frac{1}{RC}s + \frac{K}{R^2C^2}}$$

$$\text{with } \omega_o = \frac{\sqrt{K}}{RC} \quad \text{and } Q = \frac{\sqrt{K}}{1-K} . \tag{3.17}$$

The ω_o and Q sensitivities are

$$S^{\omega_o}_{C_1} = S^{\omega_o}_{C_2} = S^{\omega_o}_{K} = \frac{1}{2} \tag{3.18}$$

$$S^{\omega_o}_{R_1} = 0,\ S^{\omega_o}_{R_2} = -\frac{1}{2}(1+\frac{1}{K}) \simeq -1,\ S^{\omega_o}_{R_3} = \frac{1}{2KQ} \simeq \frac{1}{2Q} \quad \text{if } Q>>1$$

$$S^Q_{C_1} = -S^Q_{C_2} = \frac{1}{2},\quad S^Q_{R_1} = 1-\sqrt{K}Q \simeq 1-Q$$

$$S_{R_2}^{Q} = -\frac{1}{2KQ} \simeq -\frac{1}{2Q},\ S_{R_3}^{Q} = \frac{1}{2KQ} + \frac{1}{\sqrt{K}}Q \simeq Q \tag{3.19}$$

$$S_K^Q = \frac{1}{2} + \sqrt{K}\, Q \simeq \frac{1}{2} + Q. \quad \text{Thus } S_{R_b}^{Q} = -S_{R_a}^{Q} = \frac{1}{2} + Q.$$

$\Sigma S_{Z_i}^{Q} = 0$, where Z_i represents every passive element.

For the no load case (Fig. 3.5b) the ω_o and Q sensitivities are

$$S_{R_1}^{\omega_o} = S_{R_2}^{\omega_o} = S_{C_1}^{\omega_o} = S_{C_2}^{\omega_o} = -\frac{1}{2}$$

$$S_{R_1}^{Q} = -S_{R_2}^{Q} = S_{C_2}^{Q} = -S_{C_1}^{Q} = Q - \frac{1}{2} \tag{3.20}$$

$$S_K^Q = 2Q-1, \text{ thus } S_{R_b}^{Q} = -S_{R_a}^{Q} = 2Q-1.$$

Comparison of these two filters results that the Q sensitivity is lowered by a factor of 2 in the filter shown in Fig. 3.7. Since the buffer effect is obtained simultaneously with the negative resistance realization, no extra cost is imposed. The circuit in Fig. 3.8 having a negative input resistance serves as the buffer amplifier of gain 2.

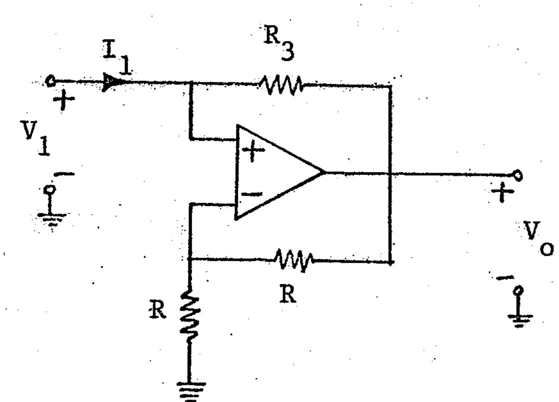

Fig. 3.8 Buffer amplifier

The complete circuit of the minimized filter is given in Fig. 3.9.

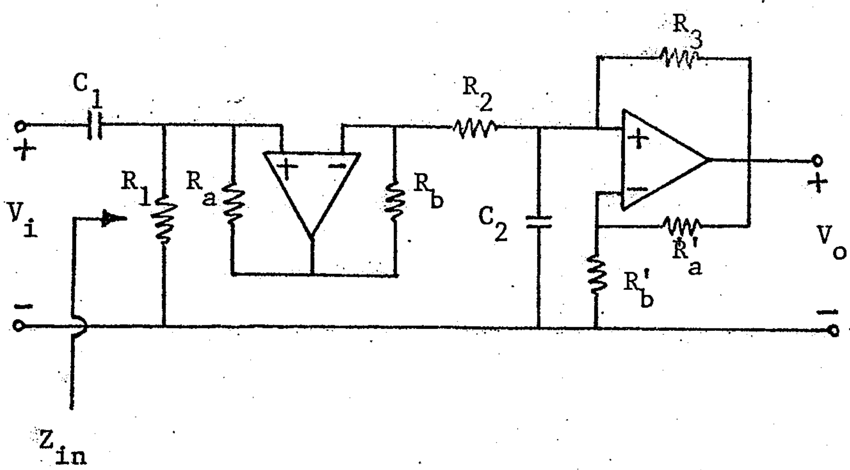

Fig. 3.9 RC-NIC realization of a second order band pass filter with minimized sensitivity

Required that: $R_1=R_2=R_3=R'_a=R'_b=R_a=R$, $R_b=R(1-\frac{1}{Q})$ and $C_1=C_2$, then

$$\frac{V_o}{V_i} = \frac{2/RC\ s}{s^2 + \frac{1-K}{RC} s + \frac{K}{R^2C^2}}$$

with $\omega_o = \frac{\sqrt{K}}{RC} = \frac{1-\frac{1}{2Q}}{RC}$ and $Q = \frac{\sqrt{K}}{1-K}$.

$$\text{Hence } \left.\frac{V_o}{V_i}\right|_{\omega_o} \simeq 2Q \quad \text{and} \quad \left.Z_{in}\right|_{\omega_o} \simeq \frac{R}{Q} \tag{3.21}$$

With the source resistance R_s as shown in Fig. 3.10 it follows that

$$\frac{V_2}{V_s} = \frac{R_1C_1s}{R_1C_1R_2C_2(1+R_sG_1-KR_sG_2)s^2+[(1-R_2G_3)(1+R_sG_1)R_1C_1+KR_1C_1R_sG_3+R_2C_2-KR_1C_2]s +1-R_2G_3+KR_1G_3} . \tag{3.22}$$

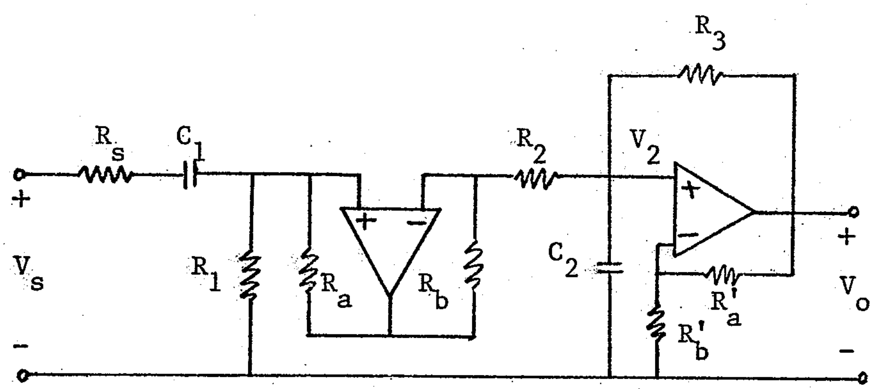

Fig. 3.10 An RC-NIC band pass filter with minimized sensitivity, non-zero source resistance.

For the equal-R, equal-C case, (3.22) is simplified as

$$\frac{V_2}{V_s} = \frac{RCs}{R^2C^2[1+R_sG(1-K)]s^2+(1-K+KR_sG)RCs+K} \quad (3.23)$$

Furthermore, the NIC conversion factor K is identically unity, and we have

$$\frac{V_2}{V_s} = \frac{s}{s^2+\frac{R_sG}{RC}s+\frac{1}{R^2C^2}} \quad (3.24)$$

where $\omega_o = \frac{1}{RC}$ and $Q = \frac{R}{R_s}$. (3.25)

It is now possible to tune ω_o and Q independently. Easy tuning of Q is insured because Q is the ratio of two resistors. The input impedance and the gain at resonance frequency are R_s and 2Q, respectively.

The ω_o and Q sensitivities are almost the same as the previous filter as follows

$$S_{C_1}^{\omega_o} = S_{C_2}^{\omega_o} = -\frac{1}{2},\ S_{R_1}^{\omega_o} = \frac{1}{2Q},\ S_{R_2}^{\omega_o} = -1 - \frac{1}{2Q},\ S_{R_3}^{\omega_o} = 0,\ S_{R_s}^{\omega_o} = 0,\ S_K^{\omega_o} = \frac{1}{2} + \frac{1}{2Q}$$

$$S_{C_1}^{Q} = -S_{C_2}^{Q} = -\frac{1}{2},\ S_{R_s}^{Q} = -1,\ S_{R_1}^{Q} = Q - \frac{1}{2Q},\ S_{R_2}^{Q} = 1 + \frac{1}{2Q},\ S_{R_3}^{Q} = -Q,\ S_K^{Q} = Q - \frac{1}{2} - \frac{1}{2Q}\ . \tag{3.26}$$

3.1.2.1 Some practical considerations

For the stability investigation under more realistic conditions we represent the operational amplifiers by a one-pole **roll off** model as shown in Fig. 3.11.

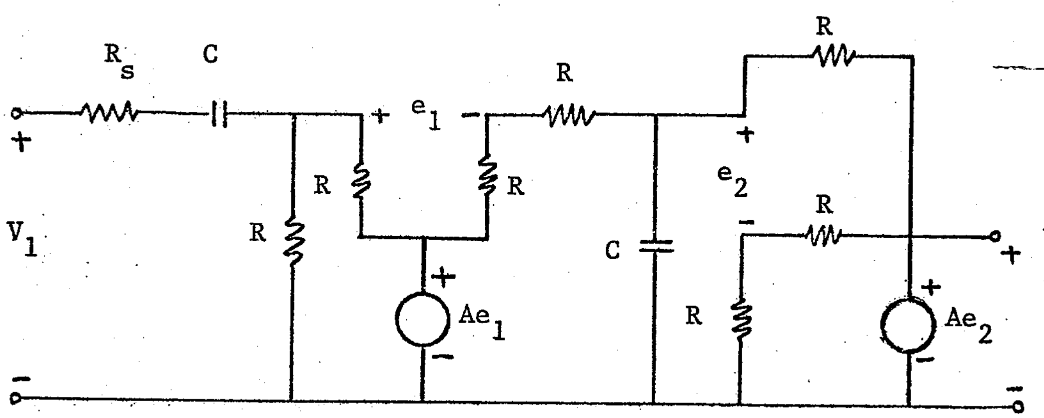

Fig. 3.11 Filter of Fig. 3.10 using one pole roll off models.

As usually the case, we assume that the gain bandwidth of the two Op-Amps are identical. The transfer function is now given as

$$\frac{V_o}{V_s} = \frac{2A}{A+2} \cdot \frac{RCs}{[1 + \frac{2}{A} + \frac{4}{A} R_s G]R^2C^2s^2 + [\frac{7}{A} + \frac{A^2+12}{A(A+2)} R_s G]RCs + \frac{A^2+12}{A(A+2)}} \tag{3.27}$$

The one-pole roll off model of the Op-Amp has the gain A which is

$$A = \frac{A_o \omega_a}{s+\omega_a} = \frac{GB}{s+\omega_a} \tag{3.28}$$

where A_o and ω_a are the gain and 3dB bandwidth under open loop situation and GB is the gain bandwidth product.

With $GB >> \omega_o >> \omega_a$, the gain may be approximated as $A \simeq \frac{GB}{s}$ and then the denominator of (3.27) can be written as

$$D = [\frac{4\omega_o^2}{GB^2} + \frac{8\omega_o^2}{QGB^2}] \frac{s^4}{\omega_o^4} + [\frac{4\omega_o}{GB} (1+ \frac{1}{Q}) + \frac{14\omega_o^2}{GB^2} + \frac{12\omega_o^2}{QGB^2}] \frac{s^3}{\omega_o^3} + [1+ \frac{7\omega_o}{GB} + \frac{12\omega_o^2}{GB^2}] \frac{s^2}{\omega_o^2}$$

$$+ \frac{1}{Q} \frac{s}{\omega_o} + 1 \,. \tag{3.29}$$

Neglecting the terms containing $[GB^2]^{-1}$: it is reduced to a cubic polynomial of

$$D = \frac{4\omega_o}{GB}(1+\frac{1}{Q})\frac{s^3}{\omega_o^3} + (1+\frac{7\omega_o}{GB})\frac{s^2}{\omega_o^2} + \frac{1}{Q}\frac{s}{\omega_o} + 1. \tag{3.30}$$

Since one of the roots is to be real we write

$$D = (s^2 + \frac{\omega_o}{Q'} s + \omega_o'^2) [\frac{4(1+\frac{1}{Q})}{\omega_o^2 GB} s + \frac{1}{\omega_o'^2}]. \tag{3.31}$$

By equating (3.31) and (3.30) we obtain

$$\frac{4(1+ \frac{1}{Q})}{\omega_o^2 GB} \frac{\omega_o'}{Q'} + \frac{1}{\omega_o'^2} = (1 + \frac{7\omega_o}{GB})\frac{1}{\omega_o^2} \tag{3.32}$$

and

$$\frac{4(1+\frac{1}{Q})}{\omega_o^2 GB} \omega_o'^2 + \frac{1}{\omega_o' Q'} = \frac{1}{Q\omega_o} . \tag{3.33}$$

where ω_o' and Q' are the deviated pole-ω_o and pole-Q.

If $\delta = \frac{\Delta\omega_o}{\omega_o} = \frac{\omega_o' - \omega_o}{\omega_o}$ and $\delta \ll 1$, then from (3.32) we have

$$\frac{4(1+\frac{1}{Q})}{Q'} \cdot \frac{(1+\delta)\omega_o}{GB} + 1-2\delta = 1+7\frac{\omega_o}{GB}. \tag{3.34}$$

The first term is negligible provided that Q has large value and therefore

$$\delta \simeq -3.5\frac{\omega_o}{GB} \tag{3.35}$$

From (3.33) we have

$$4(1+\frac{1}{Q})(1+2\delta)\frac{\omega_o}{GB} + \frac{1-\delta}{Q'} = \frac{1}{Q} \tag{3.36}$$

so that $$\frac{\Delta Q}{Q} = \frac{Q'-Q}{Q} = \frac{-\delta+4Q(1+2\delta)\frac{\omega_o}{GB}}{1-4Q(1+2\delta)\frac{\omega_o}{GB}}. \tag{3.37}$$

In a more compact form: $\frac{\Delta Q}{Q} = 4Q\frac{\omega_o}{GB}$ provided that $4Q\frac{\omega_o}{GB} \ll 1$. (3.38)

For comparison we write ω_o and Q deviations of state variable filter given in section 2.1.5

$$\frac{\Delta\omega_o}{\omega_o} \simeq -1.5\frac{\omega_o}{GB}, \qquad \frac{\Delta Q}{Q} \simeq 4Q\frac{\omega_o}{GB}. \tag{3.39}$$

It is seen that the frequency limitations of this filter are roughly comparable to state variable filter. Other practical considerations include Q-sensitivities, gain, input impedance and ease of tuning. The Q-sensitivities are relatively high and thus a high Q realization may not be stable in general, unless the resistors and capacitors are matched to have the same deviation with respect to temperature change. The input impedance is low for high-Q realizations and the loading effect on the operational amplifier may appear. The gain is 2Q which is too high for high Q realizations. Tuning is relatively easy. First we pick values for R and C to obtain desired ω_o and then adjust R_s to produce the desired Q. Section 3.4 contains experimental results which indicate the relative ease in which a fourth order BP filter can be constructed.

3.2 BP filter realization using positive feedback Q-multiplier

The block diagram of a Q-multiplier is shown in Fig. 3.12.

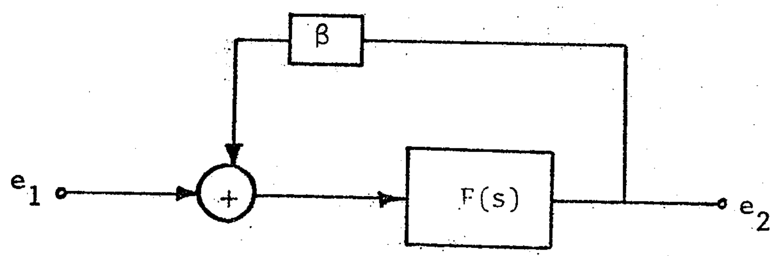

Fig. 3.12 Block diagram of a Q-multiplier

$$\text{For } F(s) = \frac{h \frac{\omega_o}{q} s}{s^2 + \frac{\omega_o}{q} s + \omega_o^2} \tag{3.40}$$

and constant β we have

$$\frac{e_2}{e_1} = \frac{F(s)}{1 - \beta F(s)} = \frac{h \frac{\omega_o}{q} s}{s^2 + (1-\beta h)\frac{\omega_o}{q} s + \omega_o^2} \tag{3.41}$$

$$\text{where } Q = \frac{q}{1-\beta h}. \tag{3.42}$$

The Q sensitivities with respect to q, β and h are

$$S_q^Q = \frac{Q}{q}$$
$$S_\beta^Q = S_h^Q = \frac{Q}{q} - 1. \tag{3.43}$$

The Q sensitivities with respect to any other parameter is calculated by the chain rule

$$S_z^Q = S_q^Q \cdot S_z^q = \frac{Q}{q} S_z^q \tag{3.44}$$

where S_z^q is the Q-sensitivity of the original filter with the quality factor q with respect to element z. From (3.44), the overall Q-sensitivities are $\frac{Q}{q}$ times larger than the Q sensitivities in the original circuit without feedback. By choosing a negative feedback type of filter for F(s) we obtain low q-sensitivities and hence reasonable values for the overall Q-sensitivities.

A negative feedback type of band pass filter with low sensitivities and least number of components is the "infinite gain multiple feedback" filter shown in Fig. 2.8(b). Since the gain is $2Q^2$ and high and also the resistance spread is of the same order, thus this filter is impractical for high Q, high order realizations. A positive feedback on this filter helps to overcome this problem as follows.

Using this filter in place of F(s) in Fig. 3.12 we produce the network given in Fig. 3.13.

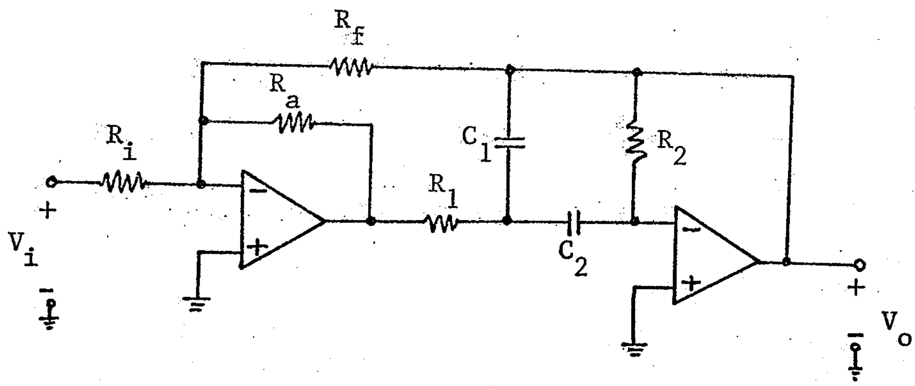

Fig. 3.13 Implementation of (3.41)

For ideal operational amplifiers and equal-C

$$\frac{V_o}{V_i} = \frac{-R_a}{R_i+R_a} \cdot \frac{h\frac{\omega_o}{q} s}{s^2+(1-\beta h)\frac{\omega_o}{q} s+\omega_o^2} \tag{3.45}$$

with $\omega_o = \frac{1}{2qR_1C}$, $q = \frac{1}{2}\sqrt{R_2/R_1}$, $\beta = \frac{R_a}{R_f}$, $h = 2q^2$.

The overall Q is $Q = \frac{q}{1-\beta h} = \frac{q}{1-2\beta q^2}$. (3.46)

The input impedance of this filter is R_i. The gain at the resonance frequency is $\frac{R_a}{R_i+R_a} \cdot 2qQ$ and thus adjustable by two resistors R_i and R_a.

The ω_o and Q sensitivities are

$$S_{R_1}^{\omega_o} = S_{R_2}^{\omega_o} = S_{C_1}^{\omega_o} = S_{C_2}^{\omega_o} = -\frac{1}{2}$$

$$S^Q_{C_1} = S^Q_{C_2} = S^Q_q \cdot S^q_{C_1} = S^Q_q \cdot S^q_{C_2} = \frac{Q}{q} \cdot 0 = 0$$

$$S^Q_{R_2} = -S^Q_{R_1} = S^Q_q \cdot S^q_{R_2} = \frac{Q}{q} \cdot \frac{1}{2} = \frac{Q}{2q} \tag{3.47}$$

$$S^Q_{R_a} = -S^Q_{R_f} = S^Q_\beta = \frac{Q}{q} - 1.$$

Thus the Q-sensitivities are less than $\frac{Q}{q}$. The value of q cannot be large because of the resistance spread in the MFB circuit. With a proper choice of Q and q however we may achieve reasonable sensitivity values.

3.2.1 Some practical considerations

The effect of nonideal operational amplifiers on the performance of the filter in Fig. 3.13 can be investigated by using one-pole roll off models for Op-Amps. As before we write $A_1(s) = A_2(s) = A(s) = \frac{GB}{s+\omega_a}$, and approximate for $\omega_a << \omega$ as $A(s) \simeq \frac{GB}{s}$. In Fig. 3.14 we obtain

$$\frac{V_o}{V_3} = \frac{-2q\omega_o s}{\frac{1}{GB}\, s^3 + [1+(2q+\frac{1}{q})\frac{\omega_o}{GB}]s^2 + [\frac{\omega_o}{q} + \frac{\omega_o^2}{GB}]s + \omega_o^2} . \tag{3.48}$$

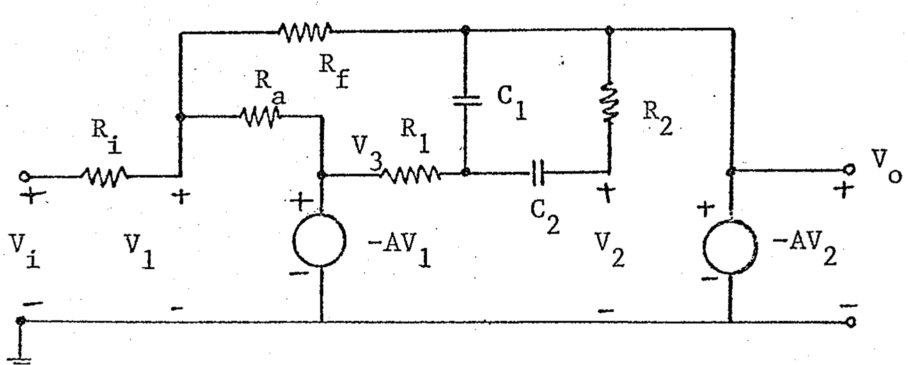

Fig. 3.14 One pole roll off models implementation of Fig. 3.13

And also

$$V_1 = V_i \frac{R_f//R_a}{R_i + R_a//R_f} + V_o \frac{R_a//R_i}{R_f+R_a//R_i} - AV_1 \frac{R_i//R_f}{R_a+R_i//R_f} . \tag{3.49}$$

The gain of this filter is usually selected to be low to allow cascade realizations in which R_a is much smaller than R_i and R_f, provided that Q is relatively high. Simplifying (3.49), we have

$$V_1 = \frac{R_a}{R_i} V_i + \frac{R_a}{R_f} V_o - AV_1 \tag{3.50}$$

or

$$V_3 = \frac{-A}{1+A}[\frac{R_a}{R_i} V_i + \frac{R_a}{R_f} V_o] . \tag{3.51}$$

Since $\frac{A}{1+A} \simeq 1$ we can substitute (3.51) in (3.48) to obtain

$$\frac{V_o}{V_i} = \frac{2\alpha q\omega_o s}{\frac{1}{GB} s^3+[1+(2q+\frac{1}{q})\frac{\omega_o}{GB}]s^2+[\frac{\omega_o}{q} + \frac{\omega_o^2}{GB} - 2\beta q\omega_o]s+ \omega_o^2} \tag{3.52}$$

where $\alpha = \frac{R_a//R_f}{R_i+R_a//R_f} \simeq \frac{R_a}{R_i}$ and $\beta = \frac{R_a//R_i}{R_f+R_a//R_i} \simeq \frac{R_a}{R_f}$.

The pole location changes when a nonideal Op-Amp is used. This change is reflected into the new pole-ω_o and pole-Q. The denominator D of (3.55) can be written in the form

$$D = (s^2 + \frac{\omega_o'}{Q'} s + \omega_o'^2)(\frac{1}{GB} s + \frac{\omega_o^2}{\omega_o'^2}) . \tag{3.53}$$

Following the same procedure as in section 3.1.2.1, we have

$$\delta \equiv \frac{\omega_o'-\omega_o}{\omega_o} = \frac{\Delta\omega_o}{\omega_o} \simeq -(q + \frac{1}{2q}) \frac{\omega_o}{GB}$$

$$\delta' \equiv \frac{Q'-Q}{Q} = \frac{\Delta Q}{Q} \simeq (2Q' \frac{\omega_o}{GB} - 1)\delta \ . \qquad (3.54)$$

For $Q' < \frac{GB}{\omega_o}$ which is usually the case it follows that $\delta' \leq \delta$.

These values are satisfactory and thus the filter is suitable for high Q, high frequency realizations. The feasibility of this circuit is verified by experimental results for cascade realizations of fourth order high-Q BP filters at medium and high frequencies, which will be presented in the next section.

3.3 Experimental results

In this section experimental results are given for two fourth order band pass filters realized by the circuits in Figs. 3.10 and 3.13 as well as a second order band pass filter realized by the circuit in Fig. 3.14. The specifications for these filters are

A - Fourth order BP:	Center frequency	= 5 kHz
	Bandwidth	= 250 Hz
	Pass band ripple	= 3 dB maximally flat
B - Fourth order BP:	Center frequency	= 5
	Bandwidth	= 100 Hz
	Pass band ripple	= 3 dB maximally flat
C - Second order BP:	Resonance frequency	= 100 kHz
	Quality factor	= 10.

In cascade realization of a fourth order BP filter, two second order sections have the following ω_o and Q [1] .

$$Q_1 = Q_2 = Q_{BP} = \frac{Q_{LP}}{\sqrt{2}}\sqrt{1 + \frac{4}{\delta^2} + \sqrt{(1+ \frac{4}{\delta^2})^2 - \frac{4}{\delta^2 Q_{LP}^2}}} \qquad (3.55)$$

$$\omega_{o1,2} = \frac{\omega_m}{2} [\delta \frac{Q_{BP}}{Q_{LP}} \pm\sqrt{(\frac{\delta Q_{BP}}{Q_{LP}})^2 - 4}]$$

where $Q_{LP} = \frac{1}{\sqrt{2}}$ for maximally flat response, $\delta = \frac{BW}{\omega_m}$ and ω_m is the center frequency. The overall gain at the center frequency is

$$\frac{K_1 K_2}{Q_{BP}^2 \delta^2} \qquad (3.56)$$

where K_1 and K_2 are the gains of each section.

3.3.1 RC-NIC filter

Filter A was realized by the circuit in Fig. 3.10, and subjected to the laboratory test. With the values of f_m = 5 kHz and BW = 250 Hz we can calculate δ, Q_{BP}, and $f_{o1,2}$

$$\delta = \frac{BW}{f_m} \div \frac{250 \text{ Hz}}{5 \cdot 10^3 \text{Hz}} = \frac{1}{20} = .05 \qquad (3.57)$$

Q_{BP} = 28.28

$f_{o1,2} = f_m[1 \pm .018]$.

For the center frequency of 4.961 kHz, the resonance frequencies of two sections become

$$f_{01} = 5.052 \text{ kHz}$$
$$\text{and } f_{02} = 4.871 \text{ kHz}. \qquad (3.58)$$

Assuming C = .01 μF, then from (3.25) we obtain

$R_1 = 3.267$ kΩ, $R_2 = 3.150$ kΩ, $R_{s_1} = 115$ Ω and $R_{s_2} = 111$ Ω.

The actual values chosen were

$R_a = R_b = R'_a = R'_b = R = 1$ kΩ ± .005 kΩ and C = 9.7 nF ± .05 nF ,

$R_2 = 3.25$ kΩ ± .05 kΩ, $R_1 = 3.37$ kΩ ± .05 kΩ, $R_{s_1} = 118$ Ω(including the 50 Ω source resistance) and $R_{s_2} = 110$ Ω. Figure 3.15 shows the resulting circuit for this filter. MC1741C Op-Amps were used throughout.

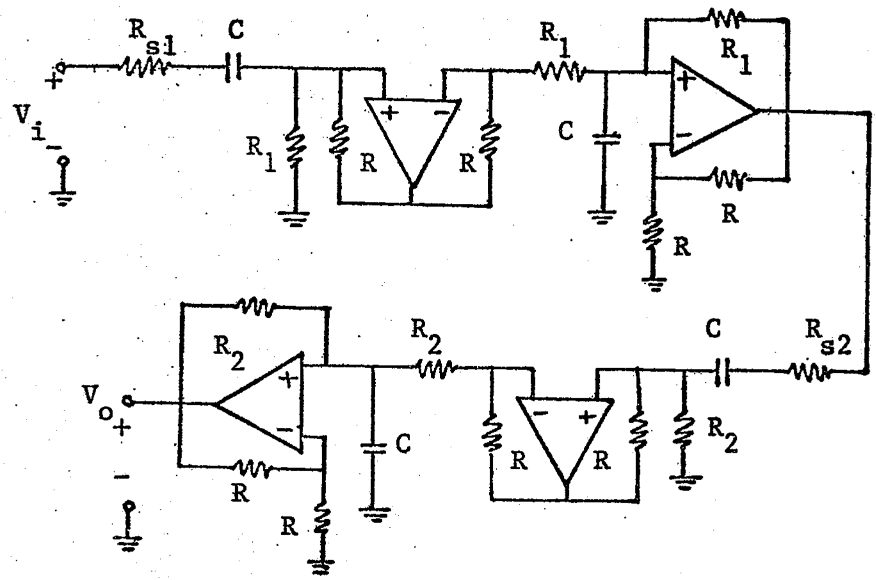

Fig. 3.15 Fourth order band pass filter

As calculated by (3.56), the overall gain becomes

$$A_{\omega_m} = \frac{2Q \cdot 2Q}{[\delta Q]^2} = \frac{4}{\delta^2} = 1600 \text{ or } 64 \text{ dB} \tag{3.59}$$

which is relatively large value.

As shown in Fig. 3.16 the experimental results closely support the theoretical prediction, the small discrepancy between the two is due to the noise at the input.

3.3.2 Q-multiplier filter

Two realizations are given for the circuit of Fig. 3.13. One is a fourth order BP with the specifications given in B and the other a second order BP with specifications given in C.

Let us first consider the fourth order BP realization. Since the center frequency for this filter is 5 kHz and bandwidth 100 Hz

$$\delta = \frac{BW}{f_m} = \frac{100}{5000} = \frac{1}{50} = .02 \tag{3.60}$$

Thus from (3.55)

$$Q_1 = Q_2 = Q_{BP} = 70.7 \tag{3.61}$$

and $f_{01,2} = f_m[1 \pm .007]$

which gives

$$\begin{aligned} f_{01} &= 5.035 \text{ kHz} \\ f_{02} &= 4.965 \text{ kHz} \\ Q_1 &= Q_2 = 70.7. \end{aligned} \tag{3.62}$$

Since $\omega_o = \frac{1}{2qRC}$, we may obtain desired ω_o by changing q.

If we choose q = 5, then

$$\frac{\Delta\omega_o}{\omega_o} \simeq -5\,\frac{5}{1000} \simeq -2.5\% \text{ and } \frac{\Delta Q}{Q} \simeq .75\% \tag{3.63}$$

From (3.47) we have

$$S^Q_{R_2} = -S^Q_{R_1} = \frac{Q}{2q} = 7,\; S^Q_{R_a} = -S^Q_{R_f} = \frac{Q}{q} - 1 = 13. \tag{3.64}$$

For the first section, with C = 10 nF, R_1 = 330 Ω and a gain of 5 we obtain

$$q_1 = \frac{1}{2\omega_{o1}R_1C} = 4.789 \quad \text{and hence} \quad R_2 = 4q_1^2R_1 = 30.27 \text{ k}\Omega$$

and

$$Q = 70.7 = \frac{q_1}{1-2\beta_1 q_1^2} \text{ which yields } \beta_1 = .02.$$

The gain of the section is 5 and hence

$$\frac{R_a}{R_i} \cdot 2qQ = 5 \quad \text{and we obtain } R_i = 133\, R_a.$$

Assuming R_a = 1 kΩ then

$$R_i = 133 \text{ k}\Omega \text{ and } R_f = 50 \text{ k}\Omega.$$

For the second section with the same C, R_1 and R_a, we obtain

$$R_2 = 31.14 \text{ k}\Omega,\ R_f = 50.8 \text{ k}\Omega \quad \text{and} \quad R_i = 137 \text{ k}\Omega.$$

The actual values of the resistors and capacitors with their tolerances are given in Table 2.

Table 2

	First Section	Second Section	
Element	Value	Value	Tolerance
R_i	133 kΩ	133 kΩ	5%
R_a	1 kΩ	1 kΩ	± .01 kΩ
R_f	42.33 kΩ	45 kΩ	± .01 kΩ
R_1	330 Ω	330 Ω	5%
R_2	28.40 kΩ	29.67 kΩ	± .01 kΩ
C	10.8 nF	10.8 nF	± .05 nF

The actual capacitances are larger than the nominal value and consequently the value of the resistor R_2 in the two sections is smaller to yield ω_o. Smaller R_2 corresponds to smaller q and smaller β and as a result R_f decreases. The gain of this filter at the center frequency is

$$A_{\omega_o} = \frac{K_1K_2}{Q^2\delta^2} = \frac{K_1K_2}{2} = \frac{5x5}{2} = 12.5 \text{ or } 21.9 \text{ dB}. \tag{3.65}$$

Fig. 3.17 confirms the close agreement between the experimental and theoretical curves.

The measured gain at an output of 7 volts peak to peak, is 21.2 dB which closely agrees with the calculated value. The limitation on the maximum output voltage is imposed only by the slew rate of the operational amplifier and the frequency of the operation. From

$$\omega V_{max} = SR \tag{3.66}$$

we have

$$V_{max} = 15.9 \text{ volts for } SR = 0.5 \text{ V/}\mu\text{s}.$$

With ±15 volt power supplies, the maximum output without distortion was measured to be 28 volts peak to peak, which confirms (3.66). Thus a good dynamic range is provided.

The second filter of interest is filter C, which is a second order band pass filter centered at a frequency of 100 kHz with a Q of 10. We start the design with the calculation of ω_o and Q deviation due to GB of the Op-Amp. From (3.55) and(3.56),we have

$$\frac{\omega_o^2}{\omega_o'^2} \simeq 1 + (2q + \frac{1}{q}) \frac{\omega_o}{GB}$$

and

$$\frac{\omega_o/GB}{1+(2q+\frac{1}{q})\frac{\omega_o}{GB}} + \frac{\omega_o/\omega_o'}{Q'} = \frac{1}{Q} + \frac{\omega_o}{GB}. \tag{3.67}$$

We have

$$\omega_o' \simeq \frac{\omega_o}{\sqrt{1+(2q+\frac{1}{q})\frac{\omega_o}{GB}}} .$$

For a typical operational amplifier like 741, the gain bandwidth product, GB is $2\pi \cdot 10^6$ rad/s, and hence

$$\frac{\omega_o}{GB} = 0.1. \tag{3.68}$$

The minimum value of $2q + \frac{1}{q}$ is $2\sqrt{2}$ for $q = \frac{1}{\sqrt{2}}$ and thus the minimum deviation factors for ω_o and Q are

$$\frac{\omega_o' - \omega_o}{\omega_o} = \delta = .12 \tag{3.69}$$

and

$$\frac{Q'-Q}{Q} \simeq -.065 , \tag{3.70}$$

respectively.

In order to circumvent the above deviations we may preadjust ω_o and Q to 112 kHz and 10.7, respectively.

With C = 1.45 nF in (3.48) and (3.49) we calculate

$$R_1 = \frac{1}{2q\omega_o C} = 680\ \Omega,$$

$$R_2 = 4q^2 R_1 = 1360\ \Omega,$$

and $\beta = \frac{1}{2q^2}(1-\frac{q}{Q}) = 0.93.$

Since $\beta = \frac{R_a}{R_f}$, we assign R_a = 1 kΩ and obtain R_f = 1.075 kΩ.

For R_i = 9.86 kΩ, the gain becomes 1.4. The slew rate effect for this filter is very important. According to (3.66) the maximum undistorted output is 0.8 volt. Since the approximation in (3.52), that $R_a << R_f$, is no longer valid then for the desired Q value of 10 R_f becomes 978 Ω. The measured peak frequency with the Q of 10 is 99.8 kHz. The gain is 1.1. Fig. 3.18 illustrates both the theoretical and experimental curves with good agreement.

The following equipments were used for the measurements of the filter characteristics.

Digital multimeter	Tektronix	DM502
Oscilloscope	Hewlett-Packard	1220A
Function generator	Tektronix	FG501
Frequency counter	Advance Instruments	TC9A
Dual power supply	Tektronix	PS503A

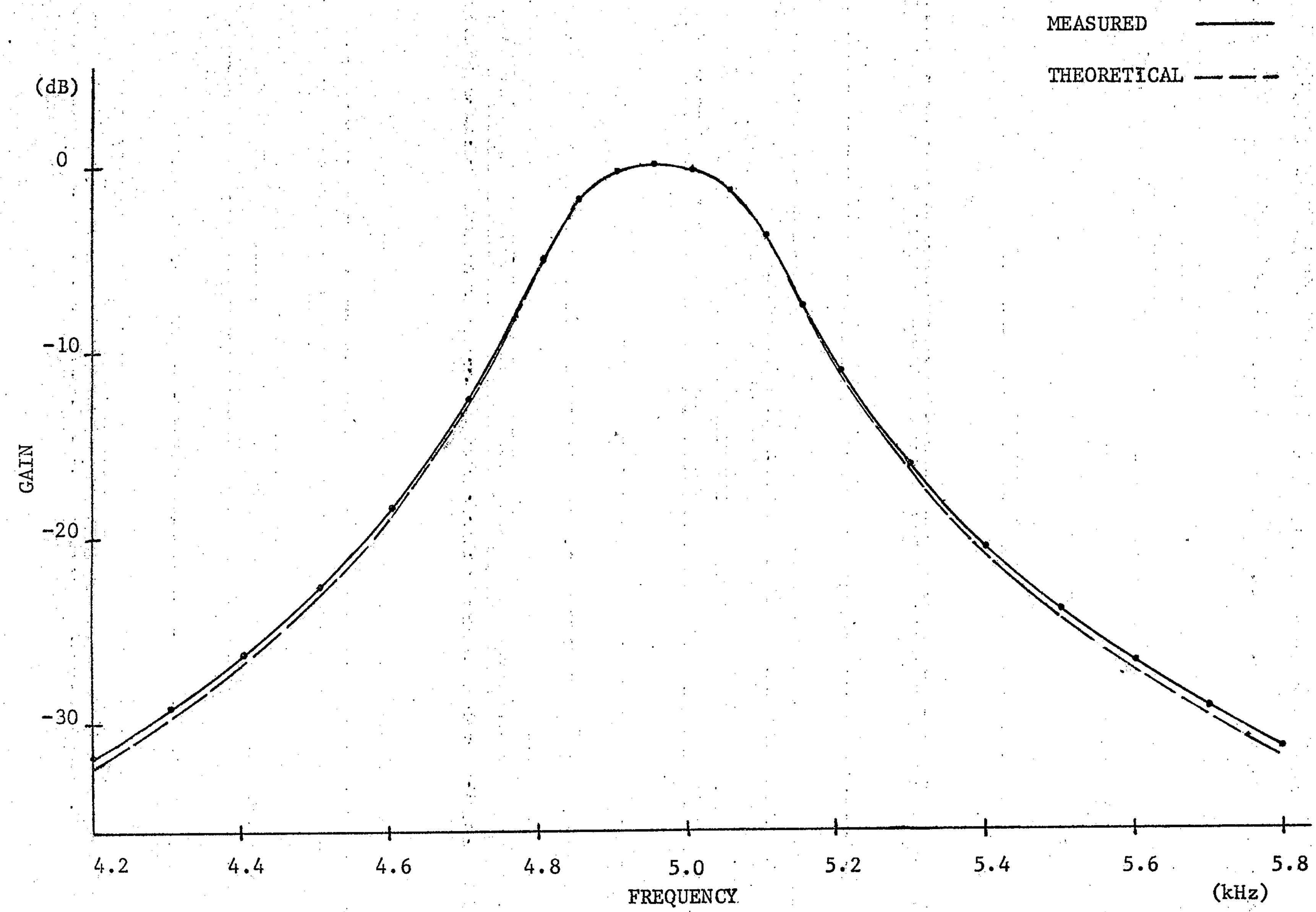

Fig. 3.16 Exprimental and theoretical curves for filter A

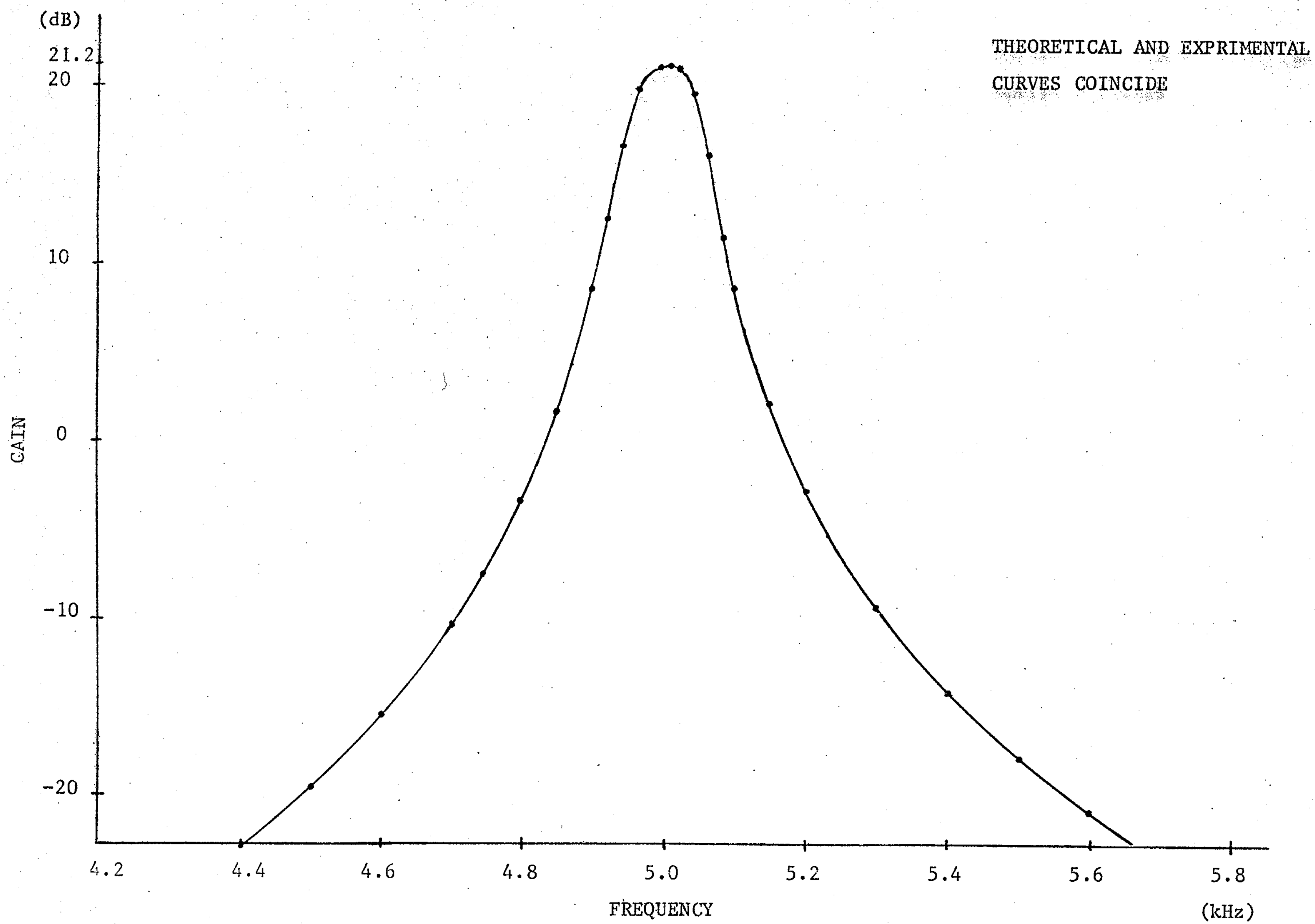

Fig. 3.17 Exprimental and theoretical curves for filter B

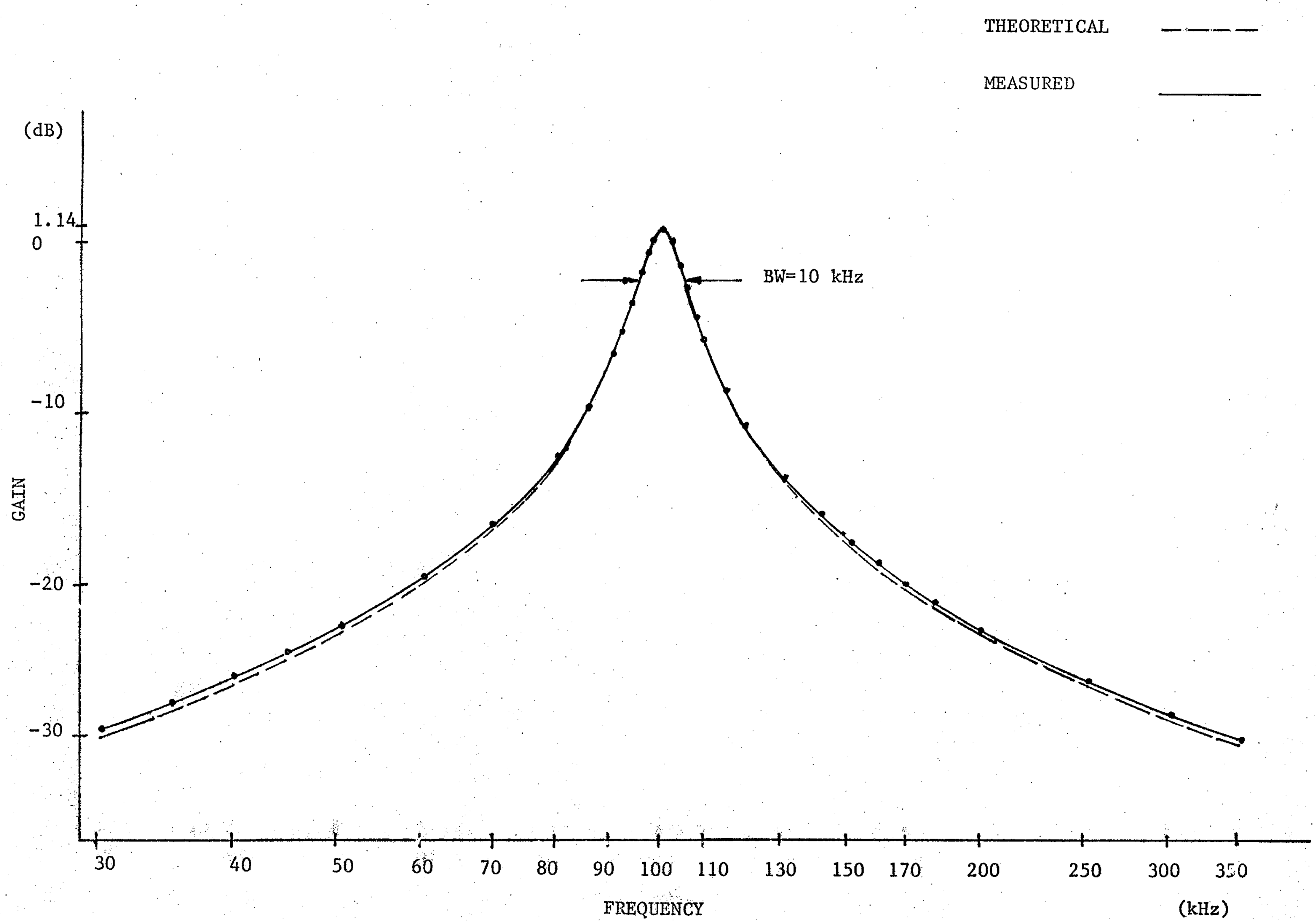

Fig. 3.18 Exprimental and theoretical curves for filter C

CHAPTER IV

CONCLUSIONS

Three second order RC-active band pass filters have been presented. The single amplifier realization, which is based on RC-VNIC technique for transfer function realization is superior to well known Sallen and Key filter in terms of the lower Q-sensitivities, higher frequency response and lower number of components. The second realization using two operational amplifiers has improved Q-sensitivities in comparison to the original RC-NIC realization. This is achieved by assigning a negative resistance for the required buffer stage. This scheme contrives for the buffer amplifier to play double roles. The third realization which is a multiple feed back filter also uses two operational amplifiers. Reasonable Q-sensitivity, high frequency response, independent tunability of ω_o, Q, R_{in}, and gain, are among the prominent features that make the high Q, high order band pass realizations practical. The experimental results are provided to illustrate the feasibility of the third filter, for high Q, high order and high center frequency band pass realizations.

REFERENCES

[1] A. Budak, "Passive and active network analysis and synthesis," pp. 579-580, Houghton, Mifflin, 1974.

[2] R.H.S. Riordan, "Simulated inductors using differential amplifiers," Electronic Letters, Vol. 3, Feb. 1967, pp. 50-51.

[3] I.M. Horowitz, "Optimization of negative-impedance conversion methods of active RC synthesis," IRE Trans. on Circuit Theory, CT-6, pp. 296-303 (Sept. 1959).

[4] D.A. Calahan, "Sensitivity minimization in active RC synthesis," IRE Trans. on Circuit Theory, CT-9, pp. 38-42 (March 1962).

[5] W.J. Kerwin, L.P. Huelsman, and R.W. Newcomb, "State variable synthesis for insensitive integrated circuit transfer functions," IEEE J. Solid-State Circuits, Vol. SC-2, pp. 87-92, Sept. 1967.

[6] A.S. Sedra and J.L. Espinoza, "Sensitivity and frequency limitations of biquadratic active filters," IEEE Trans. on Circuits and Systems, Vol. CAS-22, No. 2, Feb. 1975.

[7] G.S. Moschytz and P. Horn, "Reducing nonideal Op-Amp effects in active filters by minimizing the gain-sensitivity product (GSP)," IEEE Trans. on Circuits and Systems, Vol. CAS-24, No. 8, August 1977.

[8] A. Budak, "Passive and active network analysis and synthesis," pp. 379, Houghton, Mifflin, 1974.

[9] A.S. Sedra, "Generation and classification of single amplifier filters," Int. J. Circuit Theory Appl., Vol. 2, pp. 51-67, March 1974.

[10] A. Budak, "Passive and active network analysis and synthesis," pp. 382, Houghton, Mifflin, 1974.

[11] P.R. Geffe, "Toward high stability in active filters," IEEE Spectrum, Vol. 7, pp. 63-66, May 1970.